Geochemistry, Geochronology, and Sand Point Count Data for the Snoqualmie 7.5-minute Quadrangle, King County, Washington

by Joe D. Dragovich,
Heather A. Littke,
James H. MacDonald, Jr.,
S. Andrew DuFrane,
Megan L. Anderson,
Gregory R. Wessel,
and Renate Hartog

Geochemical Laboratory Analysts:
Diane J. Cornelius,Richard M. Conrey,
and Charles M. Knaack

WASHINGTON
DIVISION OF GEOLOGY
AND EARTH RESOURCES
Open File Report 2009-4
August 2009

This report has not been edited or reviewed for conformity with Division of Geology and Earth Resources standards and nomenclature

WASHINGTON STATE DEPARTMENT OF
Natural Resources
Peter Goldmark - Commissioner of Public Lands

DISCLAIMER
Neither the State of Washington, nor any agency thereof, nor any of their employees, makes any warranty, express or implied, or assumes any legal liability or responsibility for the accuracy, completeness, or usefulness of any information, apparatus, product, or process disclosed, or represents that its use would not infringe privately owned rights. Reference herein to any specific commercial product, process, or service by trade name, trademark, manufacturer, or otherwise, does not necessarily constitute or imply its endorsement, recommendation, or favoring by the State of Washington or any agency thereof. The views and opinions of authors expressed herein do not necessarily state or reflect those of the State of Washington or any agency thereof.

WASHINGTON DEPARTMENT OF NATURAL RESOURCES
Peter Goldmark—*Commissioner of Public Lands*

DIVISION OF GEOLOGY AND EARTH RESOURCES
David K. Norman—*State Geologist*
John P. Bromley—*Assistant State Geologist*

Washington Department of Natural Resources
Division of Geology and Earth Resources

Mailing Address:
PO Box 47007
Olympia, WA 98504-7007

Street Address:
Natural Resources Bldg, Rm 148
1111 Washington St SE
Olympia, WA 98501

Phone: 360-902-1450
Fax: 360-902-1785
E-mail: geology@dnr.wa.gov
Website: http://www.dnr.wa.gov/AboutDNR/Divisions/GER/

This and other DGER publications are available online at:
http://www.dnr.wa.gov/ResearchScience/Topics/GeologyPublicationsLibrary/Pages/pubs.aspx

The online catalog and bibliography of the Washington Geology Library is at:
http://www.dnr.wa. gov/ResearchScience/Topics/GeologyPublicationsLibrary/Pages/washbib.aspx

Suggested Citation: Dragovich, J. D.; Littke, H. A.; MacDonald, J. H., Jr.; DuFrane, S. A.; Anderson, M. L.; Wessel, G. R.; Hartog, Renate, 2009, Geochemistry, geochronology, and sand point count data for the Snoqualmie 7.5-minute quadrangle, King County, Washington: Washington Division of Geology and Earth Resources Open File Report 2009-4, 3 Microsoft Excel files with 35 p. text. [http://www.dnr.wa.gov/Publications/ger_ofr2009-4_snoqualmie_geochem.zip]

Published in the United States of America
© 2009 Washington Division of Geology and Earth Resources

Geochemistry, Geochronology, and Sand Point Count Data for the Snoqualmie 7.5-minute Quadrangle, King County, Washington

by Joe D. Dragovich[1], Heather A. Littke[1], James H. MacDonald, Jr.[2], S. Andrew DuFrane[3], Megan L. Anderson[4], Gregory R. Wessel[5], and Renate Hartog[6]

Geochemical Laboratory Analysts:
Diane J. Cornelius[7], Richard M. Conrey[7], and Charles M. Knaack[7]

[1] Washington Division of
Geology and Earth Resources
PO Box 47007
Olympia, WA 98504-7007

[2] Florida Gulf Coast University
Dept. of Marine and Ecological Science
Fort Myers, Fl 33965

[3] Washington State University
School of Earth and Environmental Sciences
Pullman, WA 99164-2812

[4] Colorado College
Department of Geology
14 E Cache La Poudre St
Colorado Springs, CO 80903

[5] King County Department of Development and
Environmental Services
900 Oakesdale Ave SW
Renton, WA 98057

[6] Pacific Northwest Seismic Network
University of Washington
PO Box 351310
Seattle, WA 98195-1310

[7] Washington State University
School of Earth and Environmental Sciences
GeoAnalytical Laboratory
PO Box 642812
Pullman, WA 99164-2812

Introduction

The reader is urged to examine the following data and analyses in conjunction with the geologic map of the Snoqualmie quadrangle (Dragovich and others, 2009a), which provides the geologic overview, geologic rock unit list and unit symbology as well as the locations of some of the sites mentioned herein including the locations of the sand point count samples, U-Pb zircon age sites, and many of the radiocarbon age sites. Geologic mapping of the Snoqualmie 7.5-minute quadrangle is part of our broader effort to provide detail geologic map information in the Snoqualmie valley area (Dragovich, 2007; Dragovich and Walsh, 2008; Dragovich and others, 2007, 2009a,b). Several electronic appendices and one figure accompany this report (Table A).

Table A. Appendices, tables, or figures in this report.

Table, appendix, or figure no.	File name	Notes
Appendix 1	a1_sand_point_count_data_snoqualmie.xls	Raw data and point count statistics and sample information for sand point count data
Appendix 2	a2_u_pb_geochronology_snoqualmie.xls	Single zircon U-Pb data, plots and sample information
Appendix 3	a3_geochemical_data_snoqualmie.xls	Geochemical data, petrography and sample information; also see Appendix 4
Appendix 4	None	Geochemical plots; also see Appendix 3

Table, appendix, or figure no.	File name	Notes
Appendix 5	None	Outcrop photos of deformational and liquefaction features in Quaternary deposits
Figure 1	None	Geochemical sample site locations in the Snoqualmie 7.5-minute quadrangle; also see location descriptions and other sample notes provided in Appendix 3
Figure 2	None	Photo of breccia and volcanic bombs site in the volcanic rocks of Snoqualmie Falls (see below)
Table 1	None	Radiocarbon ages (see below)
Table 2	None	Features of major faults (see below)

Radiocarbon Geochronology

Details about the radiocarbon ages cited in Dragovich and others (2009a) are provided in Table 1. The table also tabulates or updates information on Olympia bed samples directly west of the map area in the adjacent Fall City 7.5-minute quadrangle (Dragovich and others, 2007). The "finite ages" (44 ka or less) are correlated with the Olympia beds on the basis of age, composition and stratigraphic position. The assignment of the strata with "infinite" ages (>~44 ka) to the Olympia beds on Snoqualmie Ridge are made on the basis of composition (see sand point count data in Appendix 1) and inferred stratigraphic position in the Snoqualmie Ridge area. For example, these ancient Snoqualmie River deposits are likely stratigraphically higher than nonglacial deposits of the Whidbey Formation; that is, we found no exposures of older till or outwash of the Possession Glaciation under nonglacial deposits as was the case in the Fall City quadrangle (Dragovich and others, 2007) directly west of the map area. We cannot rule out the possibility that the intervening till and outwash were eroded before or after deposition of the younger nonglacial Olympia beds; if this was the case, then it implies considerable vertical fault offset along some strands of the Rattlesnake Mountain fault zone. For example, if the "infinite" sample 08-11L is actually from the Whidbey Formation, then Rattlesnake Mountain fault no. 11 has juxtaposed the considerably older ancient alluvium of the Whidbey Formation with ancient alluvium of the Olympia beds on Snoqualmie Ridge (see cross section B on plate 2 of Dragovich and others [2009a]). The strata containing the infinite age from borehole samples in the Snoqualmie basin east of Snoqualmie Ridge are tentatively assigned to the Whidbey Formation (see cross section A in Dragovich and others [2009a]). In this subsurface model, these organic-rich fluvial strata of the Whidbey Formation reside below Possession Glaciation outwash and represent ancient Snoqualmie River alluvium preserved in the Snoqualmie basin.

Table 1. Radiocarbon ages in the Snoqualmie and the southeastern part of the Fall City 7.5-minute quadrangles. See Dragovich and others (2007) for the location of radiocarbon sites in the Fall City quadrangle. Bold numbers provided under the "Boring or Site No." column are the well or boring numbers shown on plate 1 of Dragovich and others (2009a). "Sample elevation" gives both the boring top elevation and the radiocarbon sample elevation (provided as the elevation in parentheses). Radiocarbon surface or near surface samples have only a single sample elevation and are italicized. Olympia bed top elevation gives the local elevation of the top of the Olympia beds above the sample if applicable. AES: Associated Earth Sciences, Inc.; unit Qc_o: Olympia beds; unit Qa: Snoqualmie River alluvium (Holocene); unit Qc_w: Whidbey Formation; NA: not applicable. All elevation is measured above mean sea level.

Boring or site no.	Sample elevation (ft)	Unit Qc_o thick-ness (ft)	Olympia bed top elevation (ft)	Analyzed material	Radio-carbon age (yr B.P.)	Notes, location, and reference
ESB-1C (AES boring) (**B289B**)	417 (392)	NA	NA	wood in unit Qa	3,040 ±80	Associated Earth Sciences (1995); located 423 ft south of cross section A (site 4a) in Dragovich and others (2009a). 121°49'53.19" W, 47°32'10.23"N.
GeoEngineers (**W80**)	~438 (~320)	NA	NA	organic sediment in	5,720 (no error given)	GeoEngineers (1995); located 1,623 ft south of Borst Lake and 1,675 ft east of Highway 202; see cross

Boring or site no.	Sample elevation (ft)	Unit Qc_o thick-ness (ft)	Olympia bed top elevation (ft)	Analyzed material	Radio-carbon age (yr B.P.)	Notes, location, and reference
				unit Qaf		section A (site 5a) in Dragovich and others 2009a. Sample projected ~5,572 northwest onto Cross Section A. 121°48'57.388"W, 47°31'31.625"N.
D1B (AES boring)	860 (>800)	~134	~780-835	organic sediment in unit Qc_o	17,150 ±50	Associated Earth Sciences unpublished radiocarbon age (J. Saltonstall, AES, written commun., 2009); located 1,010 ft west of the Snoqualmie 7.5-minute quadrangle in the Fall City 7.5-minute quadrangle and ~1,154 ft northwest of cross section A in Dragovich and others (2009a). 121°52'48.916"W, 47°31'43.232"N
MW-3 (AES boring)	881 (702)	134	795	organic sediment in unit Qc_o	23,450 ±130	Associated Earth Sciences (2003); located directly south of Lake Alice and ~2,598 ft west of the Snoqualmie 7.5-minute quadrangle in the Fall City 7.5-minute quadrangle; see cross section A in Dragovich and others (2007). 121°53'12.311"W, 47°31'43.232"N
AES-1 (AES boring)	*~835*	>100	835	organic sediment in unit Qc_o	24,300 ±130	Associated Earth Sciences unpublished radiocarbon age (C. Koger, AES, written commun., 2007); surface site located 565 ft west of sec. 35, T24N R7E, in the Fall City quadrangle. Sample from organic sediments and peat below Vashon till and gravelly recessional outwash in core of anticline growth fold; see cross section A (site 1a) in Dragovich and others (2009a). 121°52'42.639"W, 47°31'35.67"N
TW-1 (AES boring)	~670 (~270)	429	559	organic sediment in unit Qc_o	24,750 ±980	Associated Earth Sciences (1987); located 4,045 ft east of the boundary with the Fall City 7.5-minute quadrangle and directly on Cross Section A (site 2a) on cross section A in Dragovich and others (2009a). Also EB-1 in reference. 121°51'35.221"W, 47°31'45.8"N.
TW-1 (AES boring)	~670 (~500)	429	559	wood in unit Qc_o	25,280 ±550	Associated Earth Sciences (1987); located 4,045 ft east of the boundary with the Fall City 7.5-minute quadrangle and directly on cross section A (site 3a) in Dragovich and others (2009a). Also EB-1 in reference. 121°51'35.221"W, 47°31'45.8"N.
TW-2 (EB-2, AES boring) (**B390**)	~830 (~530)	405	570	wood in unit Qc_o	29,460 ±1,380	Associated Earth Sciences (1987); located 982 ft east of the boundary with the Fall City 7.5-minute quadrangle; see cross section B (site 1b) in Dragovich and others (2009a). 121°52'20.565"W, 47°32'22.453"N. AES labels this boring TW-2 or EB-2 in separate publications
AES-2 (AES boring)	1000 (~970)	15+	~955	organic sediment in unit Qc_o	41,270 ±1,610	AES unpublished radiocarbon age (J. Saltonstall, AES, written commun., 2007); located 842 ft east the boundary with the Fall City 7.5-minute quadrangle and north west of Echo Lake; sample from organic sediments and peat below Vashon till and gravelly recessional outwash in the southwest part of the map area. Age may be slightly contaminated and thus infinite (note proximity of the age to the limit of the 40-44 ka for the radiocarbon age dating method). 121°52'22.282"W, 47°31'35.67"N.
GeoEngineers (**W80**)	~438 (~-51)	~200	~200	organic sediment unit Qc_w	>43,000	GeoEngineers (1995); located 1,623 ft south of Borst Lake and 1,675 ft east of Highway 202; see Cross Section A (site 6a) in Dragovich and others (2009a). Sample projected ~5,572 northwest onto cross section A and tentatively correlated with the Whidbey Formation. 121°48'57.388"W, 47°31'31.625"N. Well and boring logs indicate that this stratigraphic interval contains abundant organics (sticks, logs, peat and other organic sediments)

Boring or site no.	Sample elevation (ft)	Unit Qc_o thick-ness (ft)	Olympia bed top elevation (ft)	Analyzed material	Radio-carbon age (yr B.P.)	Notes, location, and reference
08-31C	*~555*	180	~560	dissem-inated charcoal pieces in unit Qc_o	>43,870	Surface sample (herein and Dragovich and others, 2009a); located ~1,250 ft south west of the Snoqualmie Falls and 1,953 ft west of Highway 202. Scattered small charcoal fragments within small lenses of medium sand surrounded by very dense laminated to thinly laminated mica rich fine sand to silt with low angle bedding. Laminated silt beds contain incipient flame structures at crest of outcrop; see cross section B (site 4b) in Dragovich and others (2009a). 121°50'24.769"W, 47°32'19.518"N.
08-11L	*~495*	120	~495	two ~3-cm rounded detrital wood fragments in unit Qc_o	>44,020	Surface sample (herein and Dragovich and others, 2009a); located on the west line of sec. 25 at T24N R7E. Two ~3-cm rounded detrital wood fragments found in thin lenses of medium sand; elsewhere dense laminated silt containing thin micaceous fine sand lenses, silt rip ups, and soft sediment deformation including; possible folding and vertical sand dikes; see site 3b on cross section B in Dragovich and others (2009a). 121°50'38.762"W, 47°32'17.472"N.
08-4M	*~510*	~700	~510	dissem-inated charcoal fragments in unit Qc_o	45,540 ±930	Surface sample (herein and Dragovich and others, 2009a); located 1,328 ft east of the boundary with the Fall City 7.5-minute quadrangle. Small distinct disseminated charcoal pieces along thin medium sand lenses within thick, plane bedded, laminated silt and micaceous fine to medium sand; also contains silt lenses with subtle ripples and cross-bedding defined by opaque minerals and intermittent thin beds of pebble gravel; see site 2b on cross section B in Dragovich and others (2009a). 121°52'14.698"W, 47°32'48.226"N. The proximity of the "finite" age to the upper practical limit of the radiocarbon age dating techniques suggests that this sample may be actually "infinite" as a result of contamination of the sample with traces of modern (or finite) carbon. We cannot discount this possibility but note that all the samples were extensively cleaned using a stage microscope. This process involved the removal of all suspicious charcoal fragments, rootlets and other material; as a result we suspect this is an actual finite age.

Sand Point Count Data

Here we supply sand point count data for Holocene Snoqualmie River alluvium, Olympia beds, and Possession glacial outwash. The sand point count data is presented as seven sheets within one spreadsheet (Appendix 1). This detailed sand point count data is supplemented by 53 non-point-counted sand thin section samples from various Quaternary geologic units in the Snoqualmie 7.5-minute quadrangle. The reader is urged to examine the data in conjunction with the geologic map (plate 1 of Dragovich and others, 2009a), which provides the sand sample locations. Additional sand compositional data for the adjacent Fall City and North Bend quadrangles are provided in Dragovich (2007) and Dragovich and others (2009b), respectively.

Thin-section point-count data on the sand-size fractions aids differentiation of several glacial and nonglacial units in the area (Dragovich, 2007). One important compositional discriminator for various Quaternary geologic units is the average percentage of monocrystalline quartz (Qm) *versus* quartz mica tectonite/polycrystalline quartz/chert (Qp) *versus* potassium feldspar (PF) (Also see $Qm_xQp_xPF_x$ data in Dragovich [2007].) The sand point count for the Olympia beds (unit Qc_o), Snoqualmie River alluvium (unit Qa), and outwash of the Possession Glaciation (Qgo_p) was obtained during our geologic investigation of the Snoqualmie quadrangle. Note that the "granitic lithics" point

count category includes mostly phaneritic intrusive clasts such as granite but may also include minor quartzo-feldspathic metamorphic lithic clasts such as metasandstone or quartzo-feldspathic gneiss fragments, which can be difficult to differentiate from granitic lithic grains at the scale of observation. Data show that Snoqualmie River alluvium (unit Qa) is similar modally to the ancient Snoqualmie River alluvium (unit Qc_o); Dragovich (2007) also shows that the modern Snoqualmie River sands are geochemically similar to the unit Qc_o. It is likely that the thick Olympia beds on Snoqualmie Ridge represent an "inverted basin" resulting from strike-slip faulting within the Rattlesnake Mountain fault zone (RMFZ) as discussed in Dragovich and others (2009a). In this model the thick alluvium represented by Olympia beds on Snoqualmie Ridge formed in a transtensional basin of the RMFZ. The basin was inverted when the sediments underwent uplift and folding during a later (on-going?) transpressional episode.

U-Pb LA-ICP-MS Geochronology

Introduction

We obtained four uranium-lead (U-Pb) age dates as part of our Snoqualmie quadrangle geologic mapping effort. Three of the ages are from Tertiary volcanic rocks and provide volcanic depositional ages. Two of these ages are from the volcanic rocks of Snoqualmie Falls (unit Mva_s) and one is from the volcanic rocks of Mount Persis (unit Eva_p). The fourth sample is a Western mélange belt detrital zircon age sample obtained from metasandstone. All geochronologic data including concordia plots, data tables, and sample information are supplied in electronic Appendix 2. (See Table A for electronic file names.).

Methods

Zircons for this study were analyzed for U and Pb isotopes using laser ablation inductively coupled mass spectrometry (LA-ICP-MS) at Washington State University (WSU). A full description of this method is reported in Chang and others (2006), so only a brief description is provided here.

Zircon Separation—Each sample (~10-15 kg) was crushed to fine sand-sized particles. Heavy minerals were then concentrated using an MD Mineral Technologies Gemeni Gold Table. Between each sample great care was taken to clean crushing plates and the gemini table to reduce the risk of contamination. The zircon concentrate was then passed through a 350 mm sieve and the < 350 mm fraction was cleaned by magnetic separation using a Frantz LB1. Zircons were then separated by density from the non-magnetic fraction using methylene iodide heavy liquid. From the zircon separate, ~10-50 individual zircon grains were selected from each sample and mounted in epoxy along with zircon U-Pb reference materials Peixe and FC1 (Dickinson and Gehrels, 2003; Black and others, 2004; Paces and Miller, 1993). The grain mount was polished to expose the grain centers. Regions suitable for analysis were identified from cathodoluminescence (CL) and optical imaging.

LA-ICP-MS—The analytical setup at WSU consists of a New Wave UP-213 laser ablation system interfaced with a ThermoFinnigan™ Element-2, high-resolution magnetic sector ICPMS. We operated the laser at 10 Hz repetition rate at a fluence of 10-12 J/cm^2. Laser beam size was 30 mm and pit depth was 25 mm for a typical analysis. The analysis sequence consisted of a 30s background measurement followed by an eight second laser warm-up with the shutter closed. The shutter was opened and the zircon was ablated for eight more seconds to account for sample transport time to the plasma and the time required for signal stability. Data was collected for ~46 seconds consisting of 300 scans across the masses ^{202}Hg, ^{204}(Pb + Hg), ^{206}Pb, ^{207}Pb, ^{208}Pb, ^{232}Th, ^{235}U and ^{238}U. Prior to and during each analytical session, zircon reference materials Peixe and FC1 were analyzed repeatedly and were used to externally correct the unknowns for U-Pb fractionation, mass bias, instrument drift, and to propagate uncertainties into the unknown analyses.

Data Reduction, Uncertainties, and Age Interpretation—All data were reduced offline using an Excel-based program (Chang and others, 2006) and concordia plots were generated using Isoplot (Ludwig, 2001). The uncertainties reported here are quadratic combinations of: 1) uncertainty of the measured ^{206}Pb/^{238}U and ^{207}Pb/^{206}Pb for each analysis, and 2) variance in the ^{206}Pb/^{238}U and ^{207}Pb/^{206}Pb determinations of the standards that bracket the unknowns. Overall uncertainty in age is conservatively estimated to be between 3 and 5% (1 sigma). No common Pb correction was performed on any of the analyses reported here. Isochron ages were calculated using isoplot by

anchoring to a common Pb value of 0.86 ± 0.06 and selecting the most coherent group of analyses. Terra Wasserberg Concordia plots for samples 08-44C, 08-55D, and 08-57B are provided in Appendix 2. Data used to calculate concordia intercepts are in red on these plots; the black error ellipses shown on these plots were not used for intercept calculations. Concordia ages were determined using Isoplot (Ludwig, 2001) by anchoring to a common Pb $^{207}Pb/^{206}Pb$ value of 0.86 ± 0.06. All error ellipses are 1 sigma.

Further Information and Interpretation

The volcanic rocks of Snoqualmie Falls (unit Mva_s) are named in Dragovich and others (2009a). Dragovich and others (2009b) previously obtained a U-Pb zircon age of 22.26 ±0.57 Ma from an andesite flow near the base of Snoqualmie Falls (age site 07-23A, fig. 1, appendix A in Dragovich and others, 2009b). We obtained two new U-Pb zircon ages from andesite flows along the periphery of the volcanic complex: 18.25 ±0.43 Ma (age site 08-57B, 1.5 mi downriver from Snoqualmie Falls) and 22.76 ±0.33 Ma (age site 08-44C, on Tokul Creek). These age sites are located on Plate 1 of Dragovich and others (2009a). The volcanic rocks of Snoqualmie Falls are west of the Snoqualmie Valley fault and are younger than, and not correlative with, the volcanic rocks of Mount Persis (unit Eva_p) as previously suggested by Tabor and others (1993).

We suspect that the Eocene and mid-Cretaceous zircons obtained from sample 57B and the early Oligocene, Eocene and mid-Cretaceous zircons obtained from sample 44C are assimilated accidental zircons incorporated during magmatic ascent. Using the subsurface model of Dragovich and others (2009a), candidates for assimilated underlying geologic units for sample 57B include the Western mélange belt, “basement?” undivided, the Puget Group, and (or) the Raging River Formation (Dragovich and others, 2009a). Candidates for assimilated underlying geologic units for sample 44C include rocks of the Cretaceous Western mélange belt, Oligocene-Eocene Blakeley Formation or perhaps the Eocene Puget Group. Note the correspondence between the mid-Cretaceous youngest detrital zircon ages in the Western mélange belt (sample 45J) and the assimilated zircons in samples 57B and 44C. See the Blakeley Formation (unit OEn) and Western mélange belt metasedimentary rocks (unit $KJms_w$) on cross section B (plate 2) in Dragovich and others (2009a). Western mélange belt rocks are mapped east of and below the sample site as shown on cross section B (Plate 2) of Dragovich and others (2009a). Overall, we find it compelling that the ages of the older assimilated zircons compare favorably with the general inferred ages of the strata inferred to underlie the volcanic rocks of Snoqualmie Falls on cross section B of Dragovich and others (2009a), suggesting that the accidental zircons were assimilated in the shallow part of the crust. The distinct cluster of mid-Cretaceous zircon ages in both samples 44C and 57B andesite flows might indicate (1) that the mélange belt rocks underlying the area are only mid-Cretaceous, (2) that there is an unknown mid-Cretaceous unit within the Snoqualmie basin area, and (or) (3) that mid-Cretaceous plutonic rocks were assimilated. We think it is compelling that the apparently assimilated rocks (zircons) are no older than mid-Cretaceous and suspect that this may be reflective of some fundamental difference in the age shallow basement west of the Snoqualmie Valley fault and within the Rattlesnake Mountain fault zone.

We obtained a U-Pb zircon age of 36 ±2.3 Ma (late Eocene) from a rhyolitic tuff in the volcanic rocks of Mount Persis (unit Eva_p; age site 55D on plate 1 of Dragovich and others [2009a] and in Appendix 2). Tabor and others (1993) assign a late Eocene age to the volcanic rocks of Mount Persis on the basis of a hornblende K-Ar age (38.1 Ma) and an apatite fission-track age (47.4 Ma), as well as the observation that unit Eva_p is intruded by the Index batholith (34 Ma) northeast of the map area. Lithologically and petrographically similar rhyolitic tuffs were observed by us at several sites in the volcanic rocks of Mount Persis in the Snoqualmie 7.5-minute quadrangle. Thus, the dated rhyolitic ash flow vitric tuff may be a marker bed of regional extent or the formation may contain several similar, but separate, tuff beds. The age spectra for the tuff is complex and contains zircons as old as Proterozoic. We suspect that the Eocene, Cretaceous, Paleozoic and Proterozoic zircons are a combination of assimilated accidental zircons incorporated during (1) magmatic ascent, (2) eruption, and (or) (3) catastrophic overland dispersal of the tuff whereby some of the assimilated zircons were captured during overland pyroclastic ash flow.

We obtained detrital zircon ages from a metasandstone bed in the Western melange belt. The metasandstone sample was obtained from a well-stratified and thinly to thickly bedded feldspathic metasandstone–meta-argillite sequence at age site 45J of Dragovich and others, 2009a (plate 1). We obtained a minimum U-Pb detrital zircon population

age of ~96 Ma, with a significant population at ~147 Ma; clast angularity suggests first-cycle sedimentation for most of the clasts observed in thin-section. As shown below, metasandstone geochemistry also indicates a first-cycle island arc source for a nearby sample. The minimum population age confirms that these turbidites are as young as Cretaceous as suggested by Tabor and others (1993, 2000). The occurrence of a significant U-Pb detrital zircon age population of ~147, as well as detrital grains as old as Triassic (230 Ma), indicate that the source area(s) for the turbidites are Mesozoic. The age spectra is similar to unpublished metasandstone detrital zircon data sampled from the Western mélange belt north of the map (E. H. Brown, Western Wash. Univ., retired, written commun., 2009). The provenance and outcrop stratigraphic style of the sample conforms to the accretionary prism arkosic facies of Jett and Heller (1988). These turbidites likely have a North America margin source or sources and may have originally been deposited as far south as California (Jett and Heller, 1988). The mélange belt rocks were likely was translated northward by oblique oceanic subduction in the Cretaceous. The minimum age data (1) indicates that the Western mélange belt was receiving detritus until mid-Cretaceous time, and (2) supports the contention of Tabor (1994) that the Western and Eastern mélange belts were thrust over the Northwest Cascade System (NWCS). We find it compelling that the minimum age for the metasedimentary rocks of the mélange belt roughly corresponds with the age of Northwest Cascade System thrusting. Thus we postulate: (1) that uplift was the result of mid-Cretaceous thrust emergence of the accretionary wedge rocks: (2) that the minimum age likely closely dates thrust emergence; (3) that if Tabor's (1994) model is correct then some or all of the NWCS thrust nappes may underlie the study area.

Rock Geochemistry

Introduction and Methods

New whole rock major and trace elements for 24 rock samples reported here were determined by X-ray fluorescence (XRF) and inductively coupled plasma source mass spectrometer (ICP-MS) at the Geoanalytical Laboratory at Washington State University (WSU; see Johnson and others [1999] and Knaack and others [1994] for discussion of methods). Grinding of samples for XRF and ICP-MS analyses were done at WSU, using tungsten carbide mill and iron equipment respectively (Johnson and others, 1999). Estimates of accuracy and precision for both XRF and ICP-MS at WSU are given by Johnson and others (1999) and Knaack and others (1994) respectively.

Geochemical data for the adjacent Fall City and North Bend 7.5-minute quadrangles are supplied in Dragovich (2007) and Dragovich and Walsh (2008). The locations of the geochemical samples we collected during our investigation of the Snoqualmie quadrangle are provided in Figure 1. Additionally, the geochemical data, geochemistry sample petrography and other sample information are supplied as an electronic attachment (Appendix 3). Finally, the geochemical plots (figures cited below) are supplied in a Word file attachment (Appendix 4). See Dragovich and others (2009a) for geologic symbols for the Snoqualmie quadrangle bedrock geologic units cited below. For example, $KJms_w$ is the symbol for the metasedimentary rocks of the Western mélange belt.

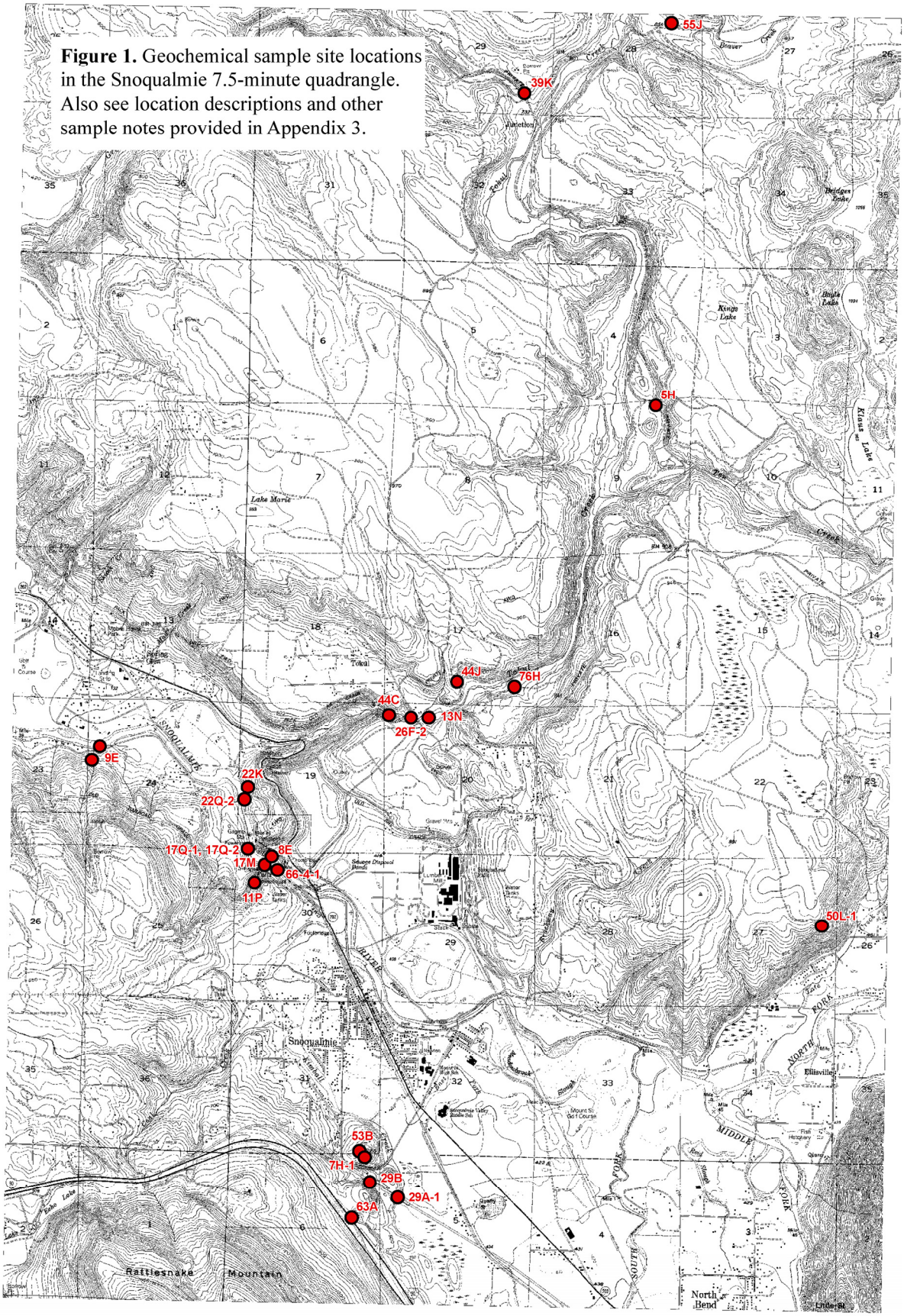

Figure 1. Geochemical sample site locations in the Snoqualmie 7.5-minute quadrangle. Also see location descriptions and other sample notes provided in Appendix 3.

Sedimentary Rock Geochemistry

Major- and trace-element geochemistry of sedimentary rocks can provide invaluable information about the original tectonic setting and the provenance of a sedimentary unit (Roser and Korsch, 1986; McLennan and others, 1993). Biogenic $CaCO_3$ or SiO_2, high concentrations of heavy minerals or quartz, as well as diagenetic reactions related to burial can affect the concentrations of elements within a sedimentary sample (Galloway, 1974; Roser and Korsch, 1986, 1988; McLennan, 1989). Thus, caution should be used when making interpretations based on geochemical analyses of sedimentary rocks, and ratios should be used whenever possible. We cannot correct for dilution resulting from $CaCO_3$ because we do not have CO_2 values for our analyses; thus, we have followed the advice of Roser and Korsch (1986, 1988) and recalculated major-element values on a CaO-free basis before plotting samples on diagrams. Two sandstones, 55J (unit OEc) and 50L (unit $KJms_w$), were chemically analyzed for this study (Appendix 3).

Both sandstones from this study display low log (SiO_2/Al_2O_3) and high log (Na_2O/K_2O) values (Appendix 4, Fig. logNa_K_logSi_Al); which is consistent with terrigenous sands that comprise greywackes (Pettijohn and others, 1972; Herron, 1988). These samples also have Th/Sc ratios below 0.6 (sample 55J = 0.11; sample 50L = 0.34) (Appendix 4, Fig. Th-Zr_Sc). Figure Th_Zr_Sc also shows that these samples have Zr/Sc ratios <10; both of these samples plot within the oceanic island arc margin field on the log (K_2O/Na_2O) *vs.* SiO_2 tectonic discrimination diagram of Roser and Korsch (1986) (Appendix 4, Fig. K/Na_Si). Chondrite normalized patterns for both of these sandstones (not shown) display an enrichment in the light rare earth elements with no pronounced negative Eu anomaly; post-Archean average shale (PAAS) normalized patterns are generally flat (not shown) with a positive Eu anomaly.

Sedimentary Rock Geochemistry—General Findings

We report only general findings here due to our small sample size (only one sample from each geologic unit). Even though the analyzed sandstones originate from two different units and are unrelated, they are chemically similar (Appendix 3). Their low Th/Sc ratios, ≤0.34, are indicative of a detrital source that is mafic in composition because Sc is enriched in mafic rocks (normal-mid-ocean ridge basalt Th/Sc = 0.003; upper continental crust Th/Sc = 1)(Appendix 4, Fig. Th-Zr_Sc)(Sun and McDonough, 1989; McLennan, 1989; McLennan and others, 1993; Floyd and others, 1991; Totten and others, 2000). These two samples were not derived from recycled sedimentary sources as indicated by their low Zr values (Appendix 4, Fig. Th-Zr_Sc) and chondrite and PAAS normalized patterns (not shown); this indicates no significant accumulation of heavy minerals (McLennan, 1989). A volcanic source is suggested for these samples because: (1) they plot within the field for oceanic island arc margins, with higher Na_2O values than PAAS, average upper continental crust, and average North American shale (Appendix 4, Fig. K/Na_Si); (2) they plot near or within the fields defined by modern back-arc basin and active margin turbidites, which are derived from active volcanic sources (Appendix 4, Fig. Th-Zr_Sc); and (3) they have a positive Eu anomaly of a PAAS normalized diagram which is the result of a source area rich in detrital feldspar (not shown). It is suggested that these samples were both derived from mafic-volcanic sources with little to no recycling. This finding is consistent with the Western mélange belt sample petrography that indicates that the metasandstones of the Western mélange belt are texturally immature first cycle sediments with a partial volcanic provenance (see "sample petrography" in Appendix 3). As a result of poor outcrops and only minor petrographic information the provenance for unit OEc remains poorly understood (Dragovich and others, 2009a).

Igneous Geochemistry

Volcanic rocks of Snoqualmie Falls (units Mva_s and $Mvbx_s$)—Unit Mva_s flow samples plot mostly within the andesite field on the total alkali-silica (TAS) diagram (Appendix 4, Fig. TAS); in addition, one sample plots near the andesite-trachyandesite boundary and another sample plots within the trachyandesite field (Appendix 4, Fig. TAS). On the AFM diagram (alkalis–FeO^T–MgO) these flows have higher FeO^T than MgO, and display a linear trend as a result of increasing Na_2O+K_2O (Appendix 4, Fig. AFM). One sample, 8E, has higher FeO^T then the other six samples (Appendix 4, Fig. AFM). Five of these flows plot within the calc-alkaline field on the K_2O–SiO_2 diagram (Appendix 4, Fig. KSi); one sample (11P) plots within the high-K field, indicating it is a high-K andesite, and sample 22K plots within the shoshonite field (Appendix 4, Fig. KSi). These flows have Sc/Pb ratios that range from ~4 to ~9 (Appendix 4, Fig. ScPbLaLu). Their chondrite normalized La/Lu values (La_N/Lu_N) are diverse, ranging

from ~6 to ~10.5 (Appendix 4, Fig. ScPbLaLu). The four breccia clasts (unit $Mvbx_s$) plot mostly within dacite field on the TAS diagram, with sample 17Q-1 plotting as an andesite (Appendix 4, Fig. TAS). These clasts display higher FeO^T than MgO, and increasing Na_2O+K_2O on the AFM diagram (Appendix 4, Fig. AFM). All of the breccia clasts plot within the calc-alkaline field on the $K_2O–SiO_2$ diagram (Appendix 4, Fig. KSi) and have Sc/Pb ratios from ~3 to ~6, and La_N/Lu_N ratios between 5 and 9 (Appendix 4, Fig. ScPbLaLu).

Snoqualmie batholith gabbro and diorite (unit MOigb)—A gabbro (sample 29B) and diorite (sample 7H-1) from the Snoqualmie batholith both plot within the basaltic andesite field on the TAS diagram (Appendix 4, Fig. TAS). These 2 samples have FeO^T/MgO ratios (~0.5), and are not enriched in Na_2O+K_2O (Appendix 4, Fig. AFM). They plot within the calc-alkaline field on the $K_2O–SiO_2$ diagram (Appendix 4, Fig. KSi). The gabbro has a Sc/Pb ratio of ~4.3 while the diorite's ratio is ~11 (Appendix 4, Fig. ScPbLaLu). These 2 samples have La_N/Lu_N ratios between 5 and 6 (Appendix 4, Fig. ScPbLaLu).

Miocene to Eocene(?) dikes (unit MEib)—Dike sample 39K plots within the basaltic andesite field and dike sample 13N plots in the andesite field on the TAS diagram (Appendix 4, Fig. TAS). Dike 39K has a lower FeO^T/MgO ratio and total Na_2O+K_2O than dike 13N (Appendix 4, Fig. AFM). Both of these dikes plot within the calc-alkaline field on the $K_2O–SiO_2$ diagram (Appendix 4, Fig. KSi). Dike 39K has a higher Sc/Pb ratio (~22) than 13N (~9); conversely, it has a lower La_N/Lu_N ratio than 13N (~2.7 and ~5.7 respectively) (Appendix 4, Fig. ScPbLaLu).

Volcanic rocks of Rattlesnake Mountain (unit $OEva_r$)—We sampled two flows from unit $OEva_r$. Both of these samples plot almost congruently in the andesite field on the TAS diagram (Appendix 4, Fig. TAS). These samples are enriched in FeO^T over MgO, and have moderate total Na_2O+K_2O (Appendix 4, Fig. AFM). They plot within the calc-alkaline field on the $K_2O–SiO_2$ diagram (Appendix 4, Fig. KSi). Their Sc/Pb ratios are between 4 and 5 and their La_N/Lu_N ratios are between 5.0 and 5.1 (Appendix 4, Fig. ScPbLaLu).

Volcanic rocks of Mount Persis of Tabor and others (1993)(unit Eva_p)—Geochemical analyses from unit Eva_p include 2 vitric tuffs (samples 5H and 44J) as well as one flow (sample 76H). The tuffs plot within the rhyolite field while the flow plots in the andesite field on the TAS diagram (Appendix 4, Fig. TAS). The tuffs are depleted in FeO^T and MgO compared to their total Na_2O+K_2O (Appendix 4, Fig. AFM). The flow has moderate FeO^T, MgO, and total Na_2O+K_2O values (Appendix 4, Fig. AFM). All three of these rocks plot within the calc-alkaline field on the $K_2O–SiO_2$ diagram (Appendix 4, Fig. KSi). Both tuffs have extremely low Sc/Pb ratios (between 0.33 and 0.45) and elevated La_N/Lu_N ratios (between 8.6 and 9) (Appendix 4, Fig. ScPbLaLu). The Sc/Pb ratio of the flow is ~9.5 while its La_N/Lu_N ratio is ~7.5 (Appendix 4, Fig. ScPbLaLu).

Western mélange belt metavolcanic rocks (unit $KJmv_w$)—For this study, two lithic metatuffaceous rocks from unit $KJmv_w$ were analyzed. Sample 26F-2 plots within the andesite field and 29A-1 plots along the basaltic andesite-andesite boundary on the TAS diagram (Appendix 4, Fig. TAS). On the AFM diagram sample 26F-2 plots with slightly higher FeO^T than MgO, and has moderately elevated Na_2O+K_2O values; conversely, sample 29A-1 is enriched in FeO^T over MgO and has much lower Na_2O+K_2O values (Appendix 4, Fig. AFM). Both of these tuffs plot within the calc-alkaline field on the $K_2O – SiO_2$ diagram (Appendix 4, Fig. KSi). Samples 26F-2 and 29A-1 have Sc/Pb and La_N/Lu_N ratios of approximately 2.7 and 3.2, plus 5.1 and 4.2, respectively (Appendix 4, Fig. ScPbLaLu).

Igneous Geochemistry—General Findings

Due to the low sample size for some geologic units only general findings can be reported here. An expanded section for the volcanic rocks of Snoqualmie Falls and their relationship to the Snoqualmie batholith is below. The igneous rocks from this study are predominantly andesite, with lesser basaltic andesite, dacite, rhyolite and one trachyandesite (Appendix 4, Fig. TAS; Fig. 1). Figures AFM and KSi (Appendix 4) reveal that these rocks are principally calc-alkaline and underwent fractional crystallization; however, a tuff from the Western mélange belt (29A-1) and a Miocene to Eocene dike (unit MEib; 39K) did not undergo large amounts of alkali crystal fractionation (Appendix 4, Fig. AFM). The La_N/Lu_N ratios (Appendix 4, Fig. ScPbLaLu) and chondrite-normalized rare earth element patterns (not shown) for these samples support this calc-alkaline and fractional crystallization interpretation; also, they suggest that these samples originated from an enriched primitive source. The $K_2O – SiO_2$ diagram (Appendix 4, Fig. KSi), where samples plot within or near the field of water-undersaturated partial melts derived from amphibolites, indicate that the enriched primitive source for these samples was mafic. The low Sc/Pb

ratios (Appendix 4, Fig. ScPbLaLu), and moderate aluminum saturation index (Appendix 3), indicate that these samples underwent minor to moderate amounts of assimilation consistent with the U-Pb zircon data (above).

Geochemical relationship of the Snoqualmie batholith to the volcanic rocks of Snoqualmie Falls

As discussed above, the volcanic rocks of Snoqualmie Falls (units Mva_s and $Mvbx_s$) and the two Snoqualmie batholith samples (unit MOigb) are calc-alkaline, originated from an enriched mafic-mantle source, and underwent varying degrees of fractional crystallization and assimilation. However, one unit Mva_s flow is a high-K andesite while another is shoshonitic (Appendix 4, Fig. KSi). Meen (1987) and Feeley and Cosca (2003) suggest that calc-alkaline to shoshonitic rocks can originate from magma fractionation and crustal assimilation, which is consistent with our interpretations above. The La_N/Lu_N ratios (Appendix 4, Fig. ScPbLaLu) indicates that these samples originated from a similar mantle source; however, the higher La_N/Lu_N ratios for two of the flows are attributed to light rare earth enrichment by fractional crystallization (Appendix 4, Fig. ScPbLaLu).

Also displayed on Figure AFM and KSi (Appendix 4) is a field for 92 Snoqualmie batholith samples from Erikson (1968, 1969). Tabor and others (1993, 2000) and Hill and Tepper (2003) note that many of Erikson's (1968, 1969) early mafic phases most likely belong to the Western mélange belt: therefore after careful sample consideration, only 5 diorite and gabbro samples from Erikson (1968, 1969) are shown on these plots (Compare Tabor and others [1993, 2000] and Erikson [1968, 1969]). These 92 samples display a calc-alkaline trend on Figure AFM, with significant overlap with the volcanic rocks of Snoqualmie Falls. The field defined by the Erikson (1968, 1969) data on Figure KSi (Appendix 4, 92 samples) predominantly overlaps with the calc-alkaline field and shows increasing K_2O with SiO_2. Furthermore, the samples also plot within or near the field of water-undersaturated partial melts derived from an area rich in amphibolite and metagreywacke source rocks, suggesting a petrogenetic origin similar to the volcanic rocks of Snoqualmie Falls (Appendix 4, Fig. KSi).

Volcanic Rocks of Snoqualmie Falls

As indicated in Dragovich and others (2009a), the volcanic rocks of Snoqualmie Falls (VRSF) are interpreted to represent a highly eroded and faulted volcanic edifice that is likely centered near Snoqualmie Falls. The exposed lithologies in this area are consistent with deposition near or on a volcano or caldera(?) and include breccias with bombs up to 9 ft in diameter (Fig. 2, below). Bombs of this size cannot be ejected a great distance from the volcanic center. Also, the VRSF complex is composed of 95 percent flows and coarse volcanic breccia and very little volcaniclastic sediment, suggesting near-source deposition. Minor lahars occur in the complex. Dragovich and others (2009a) contend that because this volcanic center is preserved in the transtensional Snoqualmie basin—and is apparently centered near the main strand of the Rattlesnake Mountain fault—that this volcanic center is structurally controlled by the Rattlesnake Mountain fault zone (RMFZ). They also contend that the magma source of the VRSF is the Snoqualmie batholith. We suspect that the batholith intruded along one or more strands of the RMFZ and that subsequent offset along various strands of the RMFZ has dissected this volcanic center. In this model, the weak cataclasitic zones of the RMFZ provided easy magma conduits for the batholith. (See unit tz of Dragovich and others, 2009a.) Here we provide some additional observations related to the stated hypotheses:

1. The gabbro bodies mapped between strands of the RMFZ have geochemical and petrographic characteristics similar to both the VRSF and the Snoqualmie batholith mapped west of the area. These bodies are correlated with the early mafic phase diorite and gabbro of the batholith, which similarly contains biotite and two pyroxenes. These similarities combined with the spatial correspondence of these gabbro bodies with the VRSF suggest a genetic relationship. (Appendices 3 and 4.)
2. The age of the Snoqualmie batholith (~17 to 25 Ma) encompasses the known age ranges of the VRSF andesite flows (18.25 ±0.43 Ma, 22.26 ±0.57, and 22.76 ±0.33 Ma). We are unsure if these andesite flows are sourced by gabbro, granodiorite, or other batholith plutonic types. Available early mafic phase ages suggest an age of around 24 Ma for most bodies, but we suspect that this plutonic complex may be the result of repeated injections of mafic magma and thus may span the majority of the age range.
3. We suspect that the andesitic, basaltic andesite to basaltic dikes found in the area are at least partially related to the VRSF and (or) the Snoqualmie batholith.
4. The age of the VRSF is similar to the Miocene Fifes Peak Formation south of Snoqualmie Falls.

5. The VRSF are preserved in a fault-bounded transtensional basin of the RMFZ that we term the Snoqualmie basin. The inferred fault boundaries of the Snoqualmie basin include the Snoqualmie Valley fault on the east and the Rattlesnake Mountain faults 1 and (or) 11 on the west (Dragovich and others, 2009a). The outlines of this basin remain broadly recognizable in the current Snoqualmie valley geography. The broad correlation of long-lived basins with some of the valley geomorphology is suggestive of continued structural control of the valley by active faulting.

Figure 2. Lithic tuff breccia with large volcanic bombs in the volcanic rocks of Snoqualmie Falls. Geologist for scale (height 5'9"). Bomb clast size is variable. The largest measured volcanic bomb occurs south of this photo and is ~ 2.5 m in diameter and suggests deposition near a volcanic edifice. Breccia clasts are mostly composed of andesite with a few lighter colored dacitic clasts (see geochemistry). A petrified log can also be found in this very thick pyroclastic breccia southeast of this site. Petrified logs and sticks are common in the breccia. Site is about 1000 ft downstream from Snoqualmie Falls on the west bank of the river at critical site no. 17Q of Dragovich and others (2009a). See sample 17Q geochemistry (this document).

Quaternary Deformation

Introduction

Obtaining direct field evidence for Holocene motion on fault strands in the region is complicated by the dense vegetative cover and urbanization. In lieu of trenching of suspected fault traces, fault investigations must rely on sparse outcroppings near topographic and geophysical lineaments or anomaly edges. Faults were mapped by Dragovich and others (2009a) on the basis of our interpretation of geophysical anomalies (figs. 3 and 4 in Dragovich and others, 2009a), geomorphologic lineaments, and stratigraphy, as well as our interpretation of deformational features observed in outcrop both locally and regionally (Dragovich and others, 2007, 2009a,b). Also, some faults are aligned with buried bedrock escarpments or lineaments including buried ancient fluvial channels, which are illuminated by depth to bedrock mapping. (fig. 2 of Dragovich and others, 2009a).

The Rattlesnake Mountain fault zone (RMFZ) is a regional strike-slip fault zone that likely correlates with the Southern Whidbey Island fault (SWIF). Individual fault strands vary from strike-slip to oblique-slip faults, although some faults with a significant vertical component of slip occur in the northeastern part of the area (Dragovich and others, 2009a). The northwest-trending Snoqualmie Valley fault and perhaps the Griffin Creek fault are interpreted to be the eastern boundary of the RMFZ in the north half of the Snoqualmie 7.5-minute quadrangle (Dragovich and others, 2009a). The Tokul Creek fault zone is a north-northeast trending fault that appears to be seismically active. Left-lateral focal mechanisms for the Tokul Creek fault zone may indicate that this fault is a conjugate to the overall right-lateral RMFZ.

Neotectonic Features

Unit Qtz is mapped around areas of prominent Quaternary deformation in Dragovich and others (2009a). These areas are interpreted to be of neotectonic origin on the basis of deformational style and common association with liquefaction features. Quaternary tectonic deformation differs from the ice-shear soft-sediment deformation noted in some advance lake and outwash deposits. Ice-shear structures at these sites have a ductile-flow aspect and display recumbent folds and other structures resulting from low-angle simple shear due to over-riding ice. Quaternary tectonic deformational features include faults, fractures, and associated liquefaction features such as flames and sand dikes. Probable tectonic deformation is recognized in both older Snoqualmie River alluvium (unit Qoa) as well as Vashon advance outwash and advance lake deposits (units Qgl_v and Qga_v) indicating that some of the deformation is likely Holocene. Digital photos at critical sites 4J, 4M, 9V, 13V, 29L, 31B, 31C, 35B, 43S, 49J, 57E, 07-46D, and 07-60P show some of the Quaternary tectonic features we observed (Appendix 5). Tectonic deformation is also supported by the spatial correspondence of the Quaternary deformation with the mapped faults; deformed Quaternary strata and liquefaction features are uncommon away from the Rattlesnake Mountain fault zone and were not observed, for example, in the northeastern part of the map area.

Deformed Olympia beds (units Qc_o and Qc_{oc}) were observed in several outcrops. For example, at critical site 29L, channel deposits are cut by northwest-trending faults that may be related to nearby, possibly active RMF no. 11A and (or) B. Fig. 6 in Appendix 5 show what may be transfer faults crossing in between RMF 11A and B at critical site 29L. Olympia beds in the Snoqualmie valley are mostly "ancient Snoqualmie River alluvium" that has likely been faulted, folded, and uplifted within the RMFZ (Dragovich and others, 2007, 2009a,b). Basin-wide deformational structures and uplift can also be inferred for unit Qc_o on the basis of (1) outcrop scale tilting, folding, fracturing and faulting, (2) unit thickness locally, and (3) elevated stratigraphic position in some areas. These beds are now elevated above the valley floor and likely represent an inverted basin or basins. In this model, the thickness of unit Qc_o along Snoqualmie Ridge (>700 ft thick) suggests original deposition in a RMFZ transtensional (extensional) basin, whereby basin inversion was accomplished through uplift and folding during a later RMFZ transpressional phase. (See 'Tertiary to Quaternary Deformation in the Study Area—Faults, Basins, and Folds' on plate 2 of Dragovich and others, 2009a.)

Major Fault Attributes

Here we document some of the attributes for the major faults mapped by Dragovich and others (2009a). The data and observations are presented as a short paragraph for each fault with some additional fault attributes documented in Table 2 (below). For further fault attribute information see Dragovich and others (2007, 2009a, b).

Rattlesnake Mountain fault no. 1 (RMF no. 1 in Table 2)—Some probable tectonic deformation along this fault particularly in areas mapped as unit Qtz (Figs. 4, 7, 8, 9, 12 in Appendix 5). A detailed gravity map done by Associated Earth Sciences (1987) shows a strong linear gravity gradient in local areas along this structure. Its coincidence with a major subsurface boundary between Snoqualmie Batholith rocks and other basement is necessary to fit geophysical modeling to linear gradients in aeromagnetic data for the quadrangle (Plate 2 of Dragovich and others, 2009a). This fault locally juxtaposes the volcanic rocks of Snoqualmie Falls against older volcanic rocks and the Puget Group. Stratigraphic relationships across this fault near Snoqualmie Falls are indicative of a long-term fault that bounds the Snoqualmie basin. The fault also bounds the Snoqualmie valley basin in the westernmost part of the Snoqualmie quadrangle and the eastern part of the Fall City quadrangle (Dragovich and others, 2007, 2009a). A straight abandoned Snoqualmie River channel follows the inferred location of the fault for about 0.5 mi southwest of Snoqualmie—although sediments proximal to this lineament are not exposed—it is possible that older alluvium (unit Qoa) was uplifted by main strand displacement in this area. Along the western boundary of the map area, the

fault also aligns with a distinct buried bedrock escarpment that bounds the Snoqualmie valley basin north of Snoqualmie Falls (see Snoqualmie valley basin in Dragovich and others, 2007). RMF no. 1 is mapped as inferred (queried), active or concealed by Dragovich and others (2009a).

Rattlesnake Mountain fault no. 3 (RMF no. 3 in Table 2)—We observed no Holocene tectonic deformation along this fault. Dragovich and others (2007) associate Olympia bed deformation and probable nearby growth folding with RMF nos. 3 and (or) 4. The fault locally bounds distinct magnetic anomaly boundaries and shows some spatial correspondence to steep, northwest-trending gravity data contours of both Dragovich and others (2009a) and Associated Earth Sciences (1987). Elsewhere, RMF no. 3 crosses the contours in the regional gravity map and is roughly coincident with an embayment in the gravity contours. (It should be noted that the exact positions of boundaries in that part of the geophysical model of Dragovich and others [2009a] are suspect because the azimuth of RMF no. 3 is oblique to the gravity contours.) This fault juxtaposes the distinctly magnetic volcanic rocks of Rattlesnake Mountain with the weakly magnetic part of the Puget Group and follows a buried lineament in the bedrock that is likely a prominent ancient channel or valley. We are uncertain of the role this fault or RMF no. 4 plays in the inversion of the Olympia beds on Snoqualmie Ridge but suspect that both RMF no. 3 and RMF no. 4 played an important structural role in the subsidence and uplift history of the ancient Snoqualmie River alluvium represented by the Olympia beds. We suspect that part of this uplift and inversion is accomplished through growth folding between RMF nos. 3 and 11. The fault bounds the Snoqualmie Valley basin northwest of the map area where this fault appears to be coincident with a significant increase of Olympia bed thickness (Dragovich and others, 2007). RMF no. 3 is mapped as concealed in the present study area.

Rattlesnake Mountain fault no. 4 (RMF no. 4 in Table 2)—This fault juxtaposes the Renton Formation against the Tukwila Formation along a broad zone of rock fault gouge in the southwestern part of the map area. We observed probable local Holocene tectonic deformation (unit Qtz) near this fault (Fig. 10 in Appendix 5; Dragovich and others, 2009a). The fault is subparallel to the glacial fluting of the Vashon glacial till. Dragovich and others (2007) extend RMF no. 3 and 4 along major creeks north of Snoqualmie Ridge and associate Olympia bed deformation and basin evolution with RMF nos. 3 and (or) 4 displacement. The fault does not bound major geophysical anomalies in the Snoqualmie quadrangle but RMF nos. 3 and (or) 4 together likely bound the Snoqualmie Valley basin northwest of the study area (Dragovich and others, 2007). RMF no. 4 is mapped as an inferred (queried) active fault or concealed fault in the present study area.

Rattlesnake Mountain fault no. 6 (RMF no. 6 in Table 2)—This fault bounds distinct magnetic anomaly boundaries of both Dragovich and others (2009a) and Associated Earth Sciences (1987). We observed likely tectonic deformation near this fault in the southern part of the study area (see critical sites 52H and 52K, and unit Qtz on plate 1 in Dragovich and others, [2009a]). However, we are uncertain if this probable tectonic deformation is the result of offset along RMF no. 6 or the nearby RMF no. 11. Sites 52K and 52H of Dragovich and others (2009a) occur in unit Qtz directly west of our inferred location of RMF no. 6. At these sites Vashon glacial till and advance lake deposits are pervaded distinct sand dikes (dikes are several centimeters thick and generally strike ~240-290° and dip 80°N to vertical). Also bedding in the glaciolacustrine deposits at these sites are likely tectonically fractured and sheared. The fault is mapped as an inferred (queried) active fault near sites 52K and 52H; otherwise the fault is mapped as concealed in the Snoqualmie 7.5-minute quadrangle. (See Dragovich and others [2009b] for further information on RMF no. 6.)

Rattlesnake Mountain fault no. 8 (RMF no. 8 in Table 2)—This fault bounds both the North Bend basin and the Snoqualmie basin in the present study area. The fault also aligns with major linear gravity boundaries in the southern part of the map area where the fault is coincident with steep buried bedrock-top contours that slope towards the North Bend basin. This fault is also near the postulated buried abandoned channel apparent on the bedrock-top contour map east of Snoqualmie Falls (Dragovich and others, 2009a). The fault is mapped as a concealed fault in the Snoqualmie quadrangle.

Rattlesnake Mountain fault no. 11 (RMF no. 11 in Table 2)—This fault is mapped as two parallel faults in the present study area (RMF no. 11A and 11B). Both of these faults appear to be associated with probable tectonic deformation (See Figs. 5, 6, 11, 13, 14, 15, 16). Also, RMF no. 11A and 11B align with short lineaments on lidar although we were unable to determine the nature of these lineaments in the field due to dense vegetative cover and recent urbanization. These faults (perhaps in concert with RMF no. 1) likely bound the inverted basin (Olympia beds) on Snoqualmie Ridge and join to bound the Snoqualmie valley basin in the west-central portion of the

Snoqualmie 7.5-minute quadrangle. The fault is mapped as an inferred (queried) active fault or concealed fault in the Snoqualmie quadrangle.

Snoqualmie Valley fault (SVF in Table 2)—This fault is inferred to be a major basin bounding fault in the study area. The fault bounds the Snoqualmie basin and likely juxtaposes the volcanic rocks of Snoqualmie Falls with older volcanic and metamorphic rocks. We speculate that the Griffin Creek fault (below) may also be part of a family of faults that bound this transtensional basin. The SVF is extended to the northwest corner of the map area based upon the geometry of geophysical anomalies; the fault appears to split magnetic highs. Some hypocenters occur near our projection of this fault into the subsurface. The fault is mostly mapped as concealed fault in the present study area. The location of the Snoqualmie Valley fault in the northwest corner of the map is poorly understood.

Griffin Creek fault (GCF in Table 2)—This fault is mapped mostly on the basis of broad lidar lineament that traverses the north-central part of the quadrangle. This lineament is slightly oblique to the distinct glacial fluting and may be tectonic and (or) have a subglacial drainage scour origin. Although the fault is not well-supported by the gravity-magnetic data—crossing magnetic gradients at a high angle—the occurrence of a possible fault scarp along a portion of the lineament suggests a locally active fault. This contention seems to be supported by the occurrence of some hypocenters near our projection of this fault into the subsurface. The disagreement between neotectonic indications and the potential field anomalies suggests the fault may be very young, with little incurred offset. The fault is mostly mapped as a concealed queried fault , and as an inferred (queried) active fault adjacent to the most prominent fault(?) scarp.

Tokul Creek fault (TCF in Table 2)—This is a major regional fault that juxtaposes basement or basement with thin overlying Tertiary volcanics against thicker Tertiary volcanic rocks that was originally mapped by Tabor and others (1993). The fault bounds low-amplitude magnetic anomalies and aligns with a possible buried ancient channel or valley outlined in the bedrock top contour map. We term a family of subparallel faults in the northeastern part of the quadrangle the Tokul Creek fault zone. Although we observed no distinct lidar lineaments or Quaternary deformation along this fault—and thus map the fault mostly as an inactive concealed fault—the occurrence of several earthquake hypocenters near our projection of the Tokul Creek fault zone in the subsurface suggests a locally active structure. Earthquake focal mechanism data suggest that this fault zone is currently accommodating left-lateral strike slip displacement (see fig. 4 on plate 2 of Dragovich and others, [2009a]).

Table 2. Major fault attributes in the Snoqualmie 7.5 minute quadrangle. Most faults are high-angle strike-slip or oblique-slip faults as discussed in Dragovich and others (2009a). Some of the mapped faults are considered probable active faults but definitive evidence of Holocene activity awaits further study (for example, detailed fault trenching). For bedrock-top contour, magnetic-gravity anomaly, and epicenter-hypocenter maps, see figures 2, 3 and 4 of Dragovich and others (2009a), respectively. Also see unit Qtz of Dragovich and others (2009a). Dragovich and others (2007, 2009b) supply further information about Rattlesnake Mountain fault zone (RMFZ) fault strands in adjacent quadrangles. Individual faults are discussed below the table. RMF: Rattlesnake Mountain fault; SVF: Snoqualmie Valley fault; GCF: Griffin Creek fault; TCF: Tokul Creek fault.

Fault Name	Associated with Tectonic Post-Glacial Deformation	Aligns with Tectonic(?) Lidar Lineaments	Bounds Magnetic and (or) Gravity Anomalies	Bounds Basin(s)	Aligns with Abandoned Channels	Associated with Earthquake Hypocenters	Notes
RMF no. 1	Probable	Probable	Locally only	Probable to Definite	Definite	Possible	See text discussion above. Also see Dragovich and others (2007, 2009b). RMFZ main strand.
RMF no. 3	None observed	None observed	Definite	Probable	Definite	Possible	See text discussion above. Also see Dragovich and others (2007, 2009b).
RMF no. 4	Probable	None observed	Locally only	Probable	Possible see RMF no. 3	Question-able	See text discussion above. Also see Dragovich and others (2007, 2009b).
RMF no. 6	Possible-probable	None observed	Definite	No	No	Possible	See text discussion above. Also see Dragovich and others (2009b).
RMF no. 8	None observed	None observed	Definite	Probable to definite	Possible	Question-able	See text discussion above. Also see Dragovich and others (2009b).
RMF no. 11	Probable	Probable	Locally only	Probable	No	Possible	See text discussion above. Also see Dragovich and others (2009b).
SVF	None observed	None observed	Definite	Probable	No	Probable	See text discussion above.
GCF	Possible	Possible	No	Possible	No	Probable	See text discussion above.
TCF	None observed	Possible	Definite	Possible	Probable	Probable to definite	See text discussion above.

REFERENCES CITED

Associated Earth Sciences, Inc., 1987, Snoqualmie Ridge project, King County, Washington—Soils, geology, geologic hazards and ground water hydrogeology: Associated Earth Sciences, Inc. [Kirkland, Wash., under contract to] Snoqualmie Ridge Associates, Inc., 2 v., 4 plates.

Associated Earth Sciences, Inc., 1995, Proposed Kimball Creek pump station, Snoqualmie, Washington—Seismic evaluation report, Snoqualmie WWTP project: Associated Earth Sciences, Inc. [prepared for KCM, Inc., project H95125D], 1 v.

Associated Earth Sciences, Inc., 2003, Proposed Snoqualmie Ridge II project—Environmental impact statement—Technical report on geology, soils, and groundwater: Associated Earth Sciences, Inc., [Kirkland, Wash., under contract to] Quadrant Corporation, 1 v.

Black, L. P.; Kamo, S. L.; Allen, C. M.; Davis, D. W.; Aleinikoff, J. N.; Valley, J. W.; Mundil, Roland; Campbell, I. H.; Korsch, R. J.; Williams, I. S.; Foudoulis, C., 2004, Improved $^{206}Pb/^{238}U$ microprobe geochronology by the monitoring of a trace-element-related matrix effect—SHRIMP, ID-TIMS, ELA-ICP-MS and oxygen isotope documentation for a series of zircon standards: Chemical Geology, v. 205, no. 1-2, p. 115-140.

Chang, Z.; Vervoort, J. D.; McClelland, W. C.; Knaack, C., 2006, U-Pb dating of zircon by LA-ICP-MS: Geochemistry, Geophysics, Geosystems, v. 7, p. 1-14.

Dickinson, W. R.; Gehrels, G. E., 2003, U-Pb ages of detrital zircons from Permian and Jurassic eolian sandstones of the Colorado Plateau, USA—Paleogeographic implications: Sedimentary Geology, v. 163, no. 1-2, p. 29-66.

Dragovich, J. D., 2007, Sand point count and geochemical data in the Fall City and Carnation 7.5-minute quadrangles, King County, Washington: Washington Division of Geology and Earth Resources Open File Report 2007-3, 2 Microsoft Excel files with 6 p. text. [http://www.dnr.wa.gov/Publications/ger_ofr2007-3_fallcity_supplement.zip]

Dragovich, J. D.; Anderson, M. L.; Walsh, T. J.; Johnson, B. L.; Adams, T. L., 2007, Geologic map of the Fall City 7.5-minute quadrangle, King County, Washington: Washington Division of Geology and Earth Resources Geologic Map GM-67, 1 sheet, scale 1:24,000. [http://www.dnr.wa.gov/Publications/ger_gm67_geol_map_fallcity_24k.zip]

Dragovich, J. D.; Littke, H. A.; Anderson, M. L.; Hartog, Renate; Wessel, G. R.; DuFrane, S. A.; Walsh, T. J.; MacDonald, J. H., Jr.; Mangano, J. F.; Cakir, Recep, 2009a, Geologic map of the Snoqualmie 7.5-minute quadrangle, King County, Washington: Washington Division of Geology and Earth Resources Geologic Map GM-75, 2 sheets, scale 1:24,000. [http://www.dnr.wa.gov/publications/ger_gm75_geol_map_snoqualmie_24k.zip]

Dragovich, J. D.; Walsh, T. J., 2008, Geochemical sample analyses of Tertiary and pre-Tertiary volcanic rocks in and around the North Bend 7.5-minute quadrangle, King County, Washington: Washington Division of Geology and Earth Resources Open File Report 2008-4, 1 Microsoft Excel file with 6 p. text. [http://www.dnr.wa.gov/Publications/ger_ofr2008-4_northbend_geochem.zip]

Dragovich, J. D.; Walsh, T. J.; Anderson, M. L.; Hartog, Renate; DuFrane, S. A.; Vervoot, Jeff; Williams, S. A.; Cakir, Recep; Stanton, K. D.; Wolff, F. E.; Norman, D. K.; Czajkowski, J. L., 2009b, Geologic map of the North Bend 7.5-minute quadrangle, King County, Washington, with a discussion of major faults, folds, and basins in the map area: Washington Division of Geology and Earth Resources Geologic Map GM-73, 1 sheet, scale 1:24,000, with 39 p. text. [http://www.dnr.wa.gov/Publications/ ger_gm73_geol_map_northbend_24k.zip]

Erikson, E. H., Jr., 1968, Petrology of the composite Snoqualmie batholith, central Cascade Mountains, Washington: Southern Methodist University Doctor of Philosophy thesis, 111 p., 1 plate.

Erikson, E. H., Jr., 1969, Petrology of the composite Snoqualmie batholith, central Cascade mountains, Washington: Geological Society of America Bulletin, v. 80, no. 11, p. 2213-2236, 1 plate.

Feeley, T. C.; Cosca, M.A., 2003, Time vs. composition trends of magmatism at Sunlight volcano, Absaroka volcanic province, Wyoming: Geological Society of America Bulletin, v. 115, no. 6, p. 714-728.

Floyd, P. A.; Shail, R.; Leveridge, B. E.; Franke, W., 1991, Geochemistry and provenance of Rhenohercynian synorogenic sandstones—Implications for tectonic environment discrimination. *In* Morton, A. C.; Todd, S. P.; Haughton, P. D. W., Developments in sedimentary provenance studies: Geological Society [London] Special Publication 57, p. 173-188.

Galloway, W. E., 1974, Deposition and diagenetic alteration of sandstone in northeast Pacific arc-related basins—Implications for greywacke genesis: Geological Society of America Bulletin, v. 85, no. 3, p. 379-390.

GeoEngineers, Inc., 1995, Report of hydrogeologic services, south well field characterization, Snoqualmie, Washington: GeoEngineers [for Puget Western, Inc.], 1 v.

Gromet, L. P.; Haskin, L. A.; Korotev, R. L.; Dymek, R. F., 1984, The "North American shale composite"—Its compilation, major and trace element characteristics: Geochimica et Cosmochimica Acta, v. 48, no. 12, p. 2469-2482.

Herron, M. M., 1988, Geochemical classification of terrigenous sands and shales from core or log data: Journal of Sedimentary Petrology, v. 58, no. 5, p. 820-829.

Hill, K. S.; Tepper, J. H., 2003, Petrology of mafic plutons in the Snoqualmie batholith, north Cascades, Washington: Geological Society of America Abstracts with Program, v. 35, no. 4, p. 4.

Jett, G. A.; Heller, P. L., 1988, Tectonic significance of polymodal compositions in mélange sandstones, western mélange belt, north Cascade Range, Washington: Journal of Sedimentary Petrology, v. 58, no. 1, p. 52-61.

Johnson, D. M.; Hooper, P. R.; Conrey, R. M., 1999, XRF analysis of rocks and minerals for major and trace elements on a single low dilution Li-tetraborate fused bead: Advances in X-ray Analysis, v. 41, p. 843-867. [http://www.wsu.edu/~geolab/note/V41_91.pdf]

Knaack, C.; Cornelius, S.; Hooper, P., 1994, Trace element analysis of rocks and minerals by ICP/MS: Department of Geology, Washington State University Open-File Report, December 1994, 18 p.

Le Maitre, R. W., ed., 2002, Igneous rocks—A classification and glossary of terms; 2nd ed.: Cambridge University Press [Cambridge, U.K.], 236 p.

Ludwig, K. R., 2001, Isoplot/EX rev2.49—A geochronological toolkit for Microsoft Excel: Berkeley Geochronology Center, Special Publication 1a, p. 1-58.

Meen, J. K, 1987, Formation of shoshonites from calc-alkaline basalt magmas—Geochemical and experimental constraints from the type locality: Contributions to Mineralogy and Petrology, v. 97, no. 3, p. 333-351.

McLennan, S. M., 1989, Rare earth elements in sedimentary rocks—Influence of provenance and sedimentary processes: Reviews in Mineralogy and Geochemistry, v. 21, no. 1, p. 169-200.

McLennan, S. M., 2001, Relationships between the trace element composition of sedimentary rocks and upper continental crust: Geochemistry, Geophysics, Geosystems - G 3, 2, p. 2000GC000109.

McLennan, S. M.; Hemming, S.; McDaniel; D. K.; Hanson, G. N., 1993, Geochemical approaches to sedimentation, provenance, and tectonics. *In* Johnson, M. J.; Basu, A., eds., Processes controlling the composition of clastic sediments: Geological Society of America Special Paper 284, p. 21-40.

McLennan, S. M.; Taylor, S. R.; McCulloch, M. T.; Maynard, J. B., 1990, Geochemical and Nd-Sr isotopic composition of deep-sea turbidites—Crustal evolution and plate tectonic associations: Geochimica et Cosmochimica Acta, v. 54, no. 7, p. 2015-2050.

Paces, J. B.; Miller J. D., Jr., 1993, Precise U-Pb ages of Duluth complex and related mafic intrusions, northeastern Minnesota—Geochronological insights to physical, petrogenetic, paleomagnetic, and tectonomagmatic processes associated with the 1.1 Ga midcontinent rift system: Journal of Geophysical Research, v. 98, no. B8, p. 13,997-14,013.

Pettijohn, F. J.; Potter, P. E.; Siever, Raymond, 1973, Sand and sandstone: Springer-Verlag [New York], 618 p.

Roser, B. P.; Korsch, R. J., 1986, Determination of tectonic setting of sandstone-mudstone suites using SiO_2 content and K_2O/Na_2O ratio: Journal of Geology, v. 94, no. 5, p. 635-650.

Roser, B. P.; Korsch, R. J., 1988, Provenance signatures of sandstone-mudstone suites determined using discriminant function analysis of major-element data: Chemical Geology, v. 67, no. 1-2, p. 119-139.

Sisson, V. B.; Poole, A. R.; Harris, N. R.; Burner, H. C.; Pavlis, T. L.; Copeland, P.; Donelick, R. A.; McLelland, W. C., 2003, Geochemical and geochronologic constraints for genesis of a tonalite-trondhjemite suite and associated mafic intrusive rocks in the eastern Chugach Mountains, Alaska—A record of ridge-transform subduction. *In* Sisson, V. B.; Roeske, S. M.;d Pavlis, T. L., Geology of a transpressional orogen developed during ridge-trench interaction along the North Pacific margin: Boulder, Colorado, Geological Society of America Special Paper 371, p. 293-326.

Sun, S. S.; McDonough, W. F., 1989, Chemical and isotopic systematics of oceanic basalts—Implications for mantle composition and processes. *In* Saunders, A. D.; Norry, M. J., eds., Magmatism in the ocean basins: Geological Society Special Publications, no. 42, p. 313-345.

Tabor, R. W., 1994, Late Mesozoic and possible early Tertiary accretion in western Washington State—The Helena-Haystack mélange and the Darrington–Devils Mountain fault zone: Geological Society of America Bulletin, v. 106, no. 2, p. 217-232, 1 plate.

Tabor, R. W.; Frizzell, V. A., Jr.; Booth, D. B.; Waitt, R. B., 2000, Geologic map of the Snoqualmie Pass 30 x 60 minute quadrangle, Washington: U.S. Geological Survey Geologic Investigations Series Map I-2538, 1 sheet, scale 1:100,000, with 57 p. text. [http://geopubs.wr. usgs.gov/i-map/i2538/]

Tabor, R. W.; Frizzell, V. A., Jr.; Booth, D. B.; Waitt, R. B.; Whetten, J. T.; Zartman, R. E., 1993, Geologic map of the Skykomish River 30- by 60-minute quadrangle, Washington: U.S. Geological Survey Miscellaneous Investigations Series Map I-1963, 1 sheet, scale 1:100,000, with 42 p. text. [http://geopubs.wr.usgs.gov/i-map/i1963/]

Totten, M. W.; Hanan, M. A.; Weaver, B. L., 2000, Beyond whole-rock geochemistry of shales—The importance of assessing mineralogic controls for revealing tectonic discriminants of multiple sediment sources for the Ouachits Mountain flysch deposits: Geological Society of America Bulletin, v. 112, no. 7, p. 1012-1022.

Appendix 1. Sand Point Count Data

See attached file: a1_sand_point_count_data_snoqualmie.xls.

Appendix 2. Uranium-Lead Geochronology

See attached file: a2_u_pb_geochronology_snoqualmie.xls.

Appendix 3. Geochemical Data

See attached file: a3_geochemical_data_snoqualmie.xls.

Appendix 4. Geochemical Plots

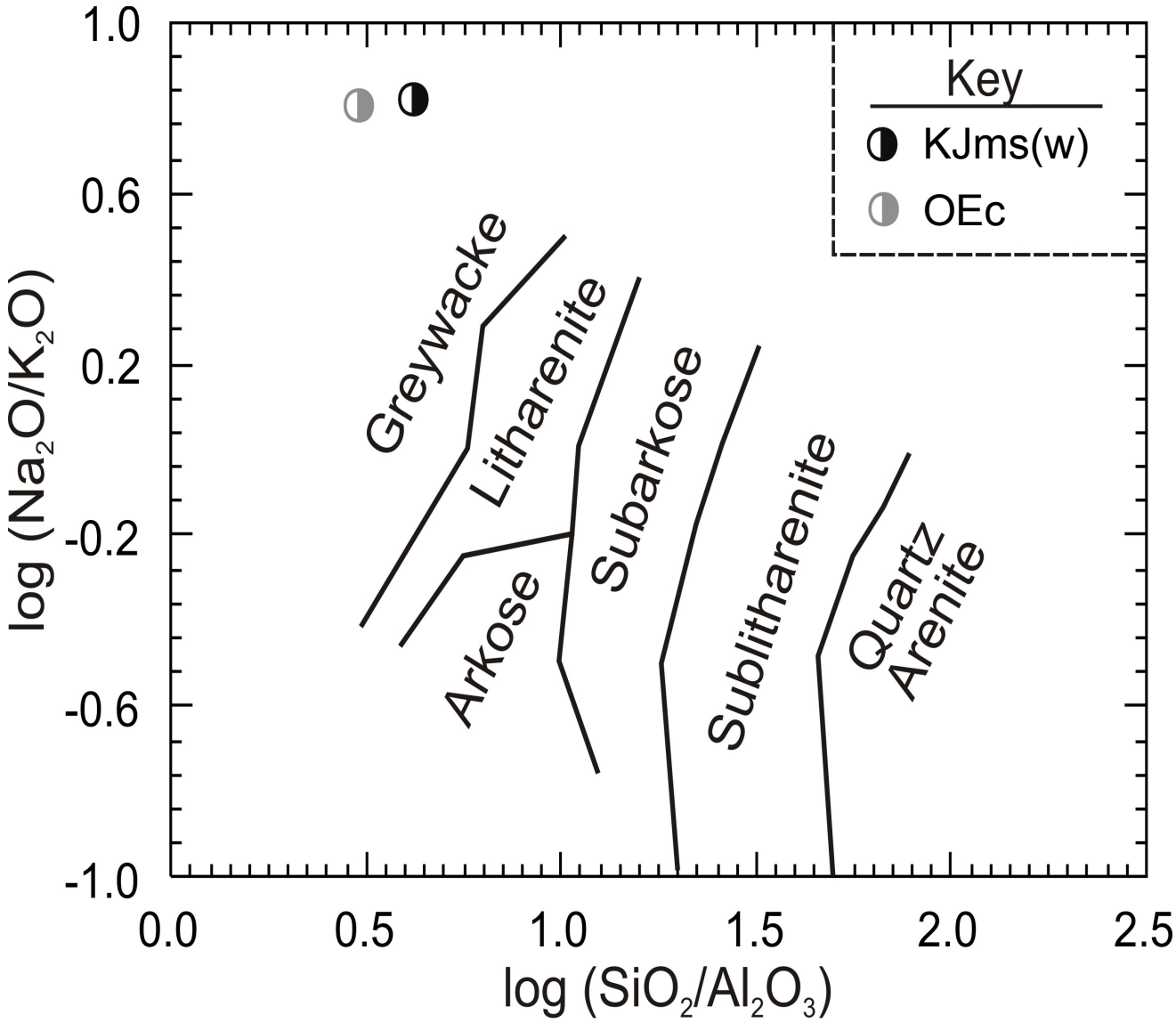

Figure logNa_K_logSi_Al. Proposed classification for terrigenous sandstones based on the log(Na_2O/K_2O) *vs.* log(SiO_2/Al_2O_3) values: from Pettijohn and others (1972), with field boundaries modified by Herron (1988). Units include the Western mélange belt metasedimentary rocks (unit $KJms_w$) and undivided Oligocene–Eocene continental sedimentary rocks (unit OE_c).

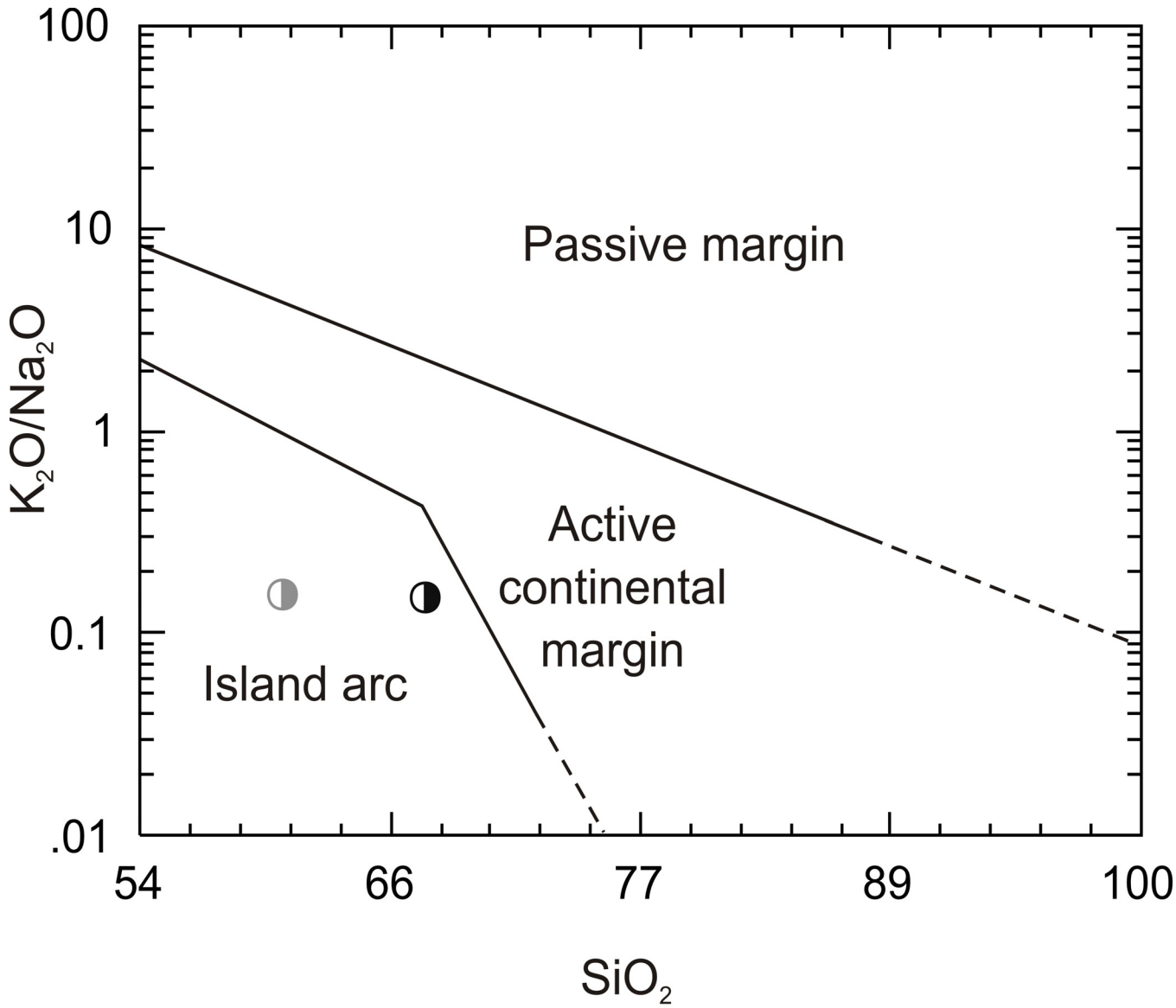

Figure K/Na_Si. Tectonic discrimination diagram for depositional environments for sandstones and argillites from Roser and Korsch (1986). Island arc = deposition in oceanic island arc margins. Also plotted are the average values for North American shale composite (NASC), post-Archean Australian shale composite (PAAS), upper continental crust (UC; Gromet and others, 1984; McLennan, 1989; McLennan, 2001). Symbols are the same as Figure logNa_K_logSi_Al. Units include the Western mélange belt metasedimentary rocks (unit $KJms_w$) and undivided Oligocene–Eocene continental sedimentary rocks (unit OE_c).

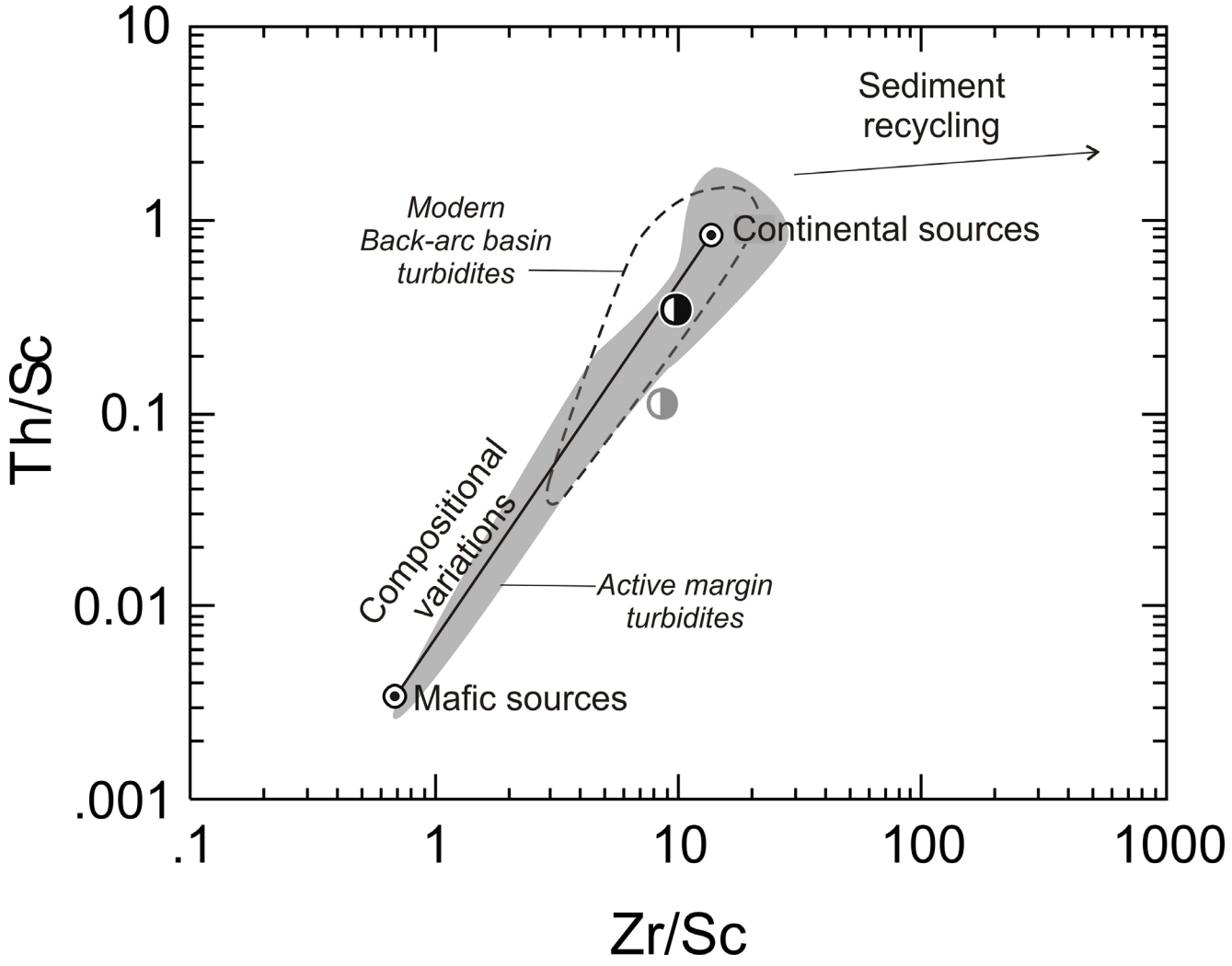

Figure Th-Zr_Sc. Th/Sc versus Zr/Sc plot modified from McLennan and others (1993) by the addition of average upper continental crust (representing cratonic sources; McLennan, 2001) and the field for modern back arc basin turbidities (McLennan and others, 1990). Symbols are the same as in Figure logNa_K_logSi_Al. Units include the Western mélange belt metasedimentary rocks (unit $KJms_w$) and undivided Oligocene–Eocene continental sedimentary rocks (unit OE_c).

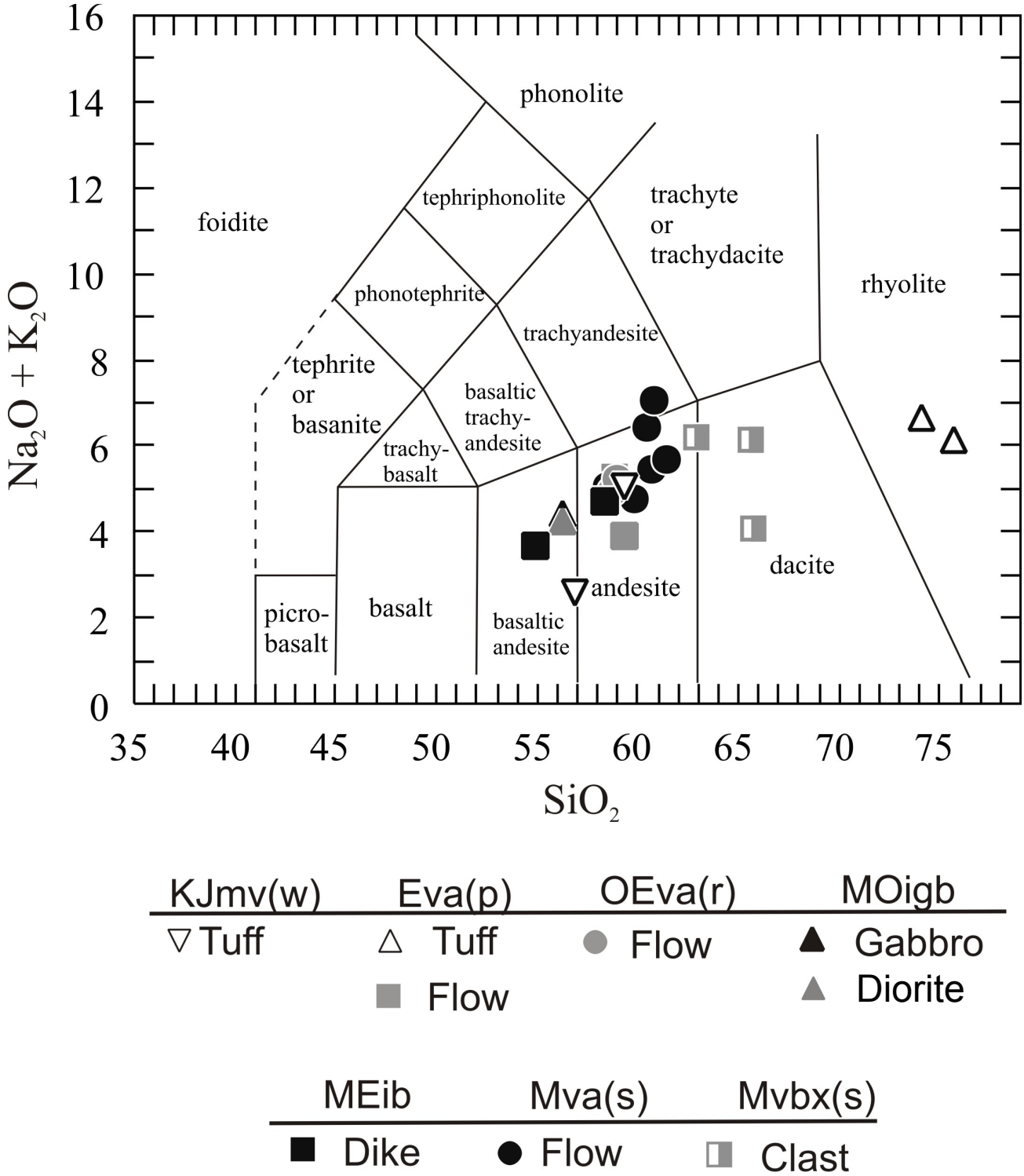

Figure TAS. Total alkali-silica (TAS) chemical classification diagram for aphanitic igneous rocks from the Snoqualmie quadrangle. Modified from Le Maitre (2002). Geologic units include the Western mélange belt metavolcanic rocks (unit $KJmv_w$), volcanic rocks of Mount Persis (unit Eva_p), volcanic rocks of Rattlesnake Mountain (unit $OEva_r$), Snoqualmie batholith gabbro (unit MOigb), Miocene to Eocene dikes (unit MEib), and the volcanic rocks of Snoqualmie Falls (units Mva_s and $Mvbx_s$). Clasts in the breccia are from unit $Mvbx_s$.

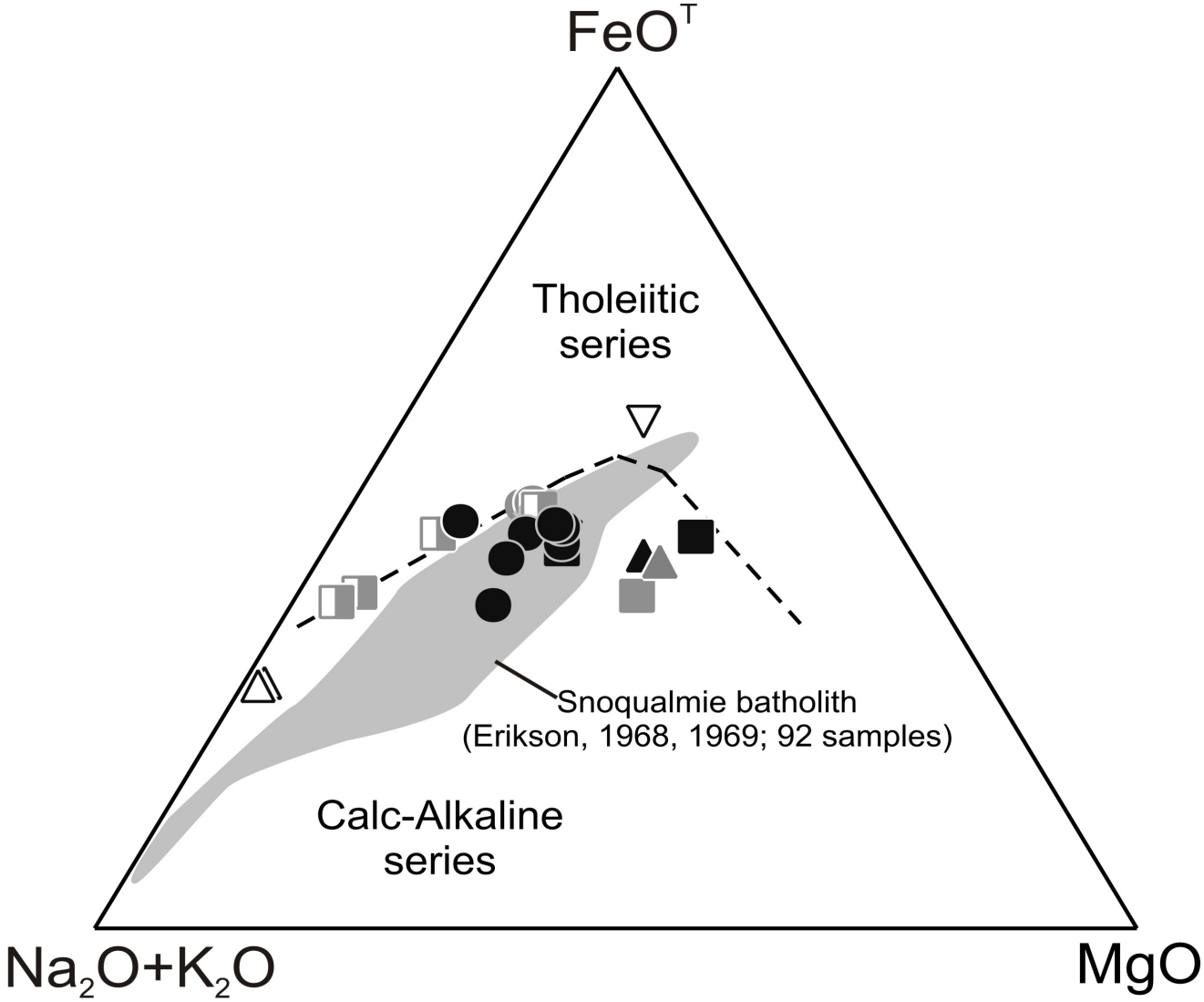

Figure AFM. AFM (Na_2O+K_2O – total iron as FeO^T – MgO) diagram for igneous rocks from the Snoqualmie quadrangle. Also plotted are 92 samples from the Snoqualmie batholith (Erikson, 1968, 1969). Symbols are the same as in Figure TAS.

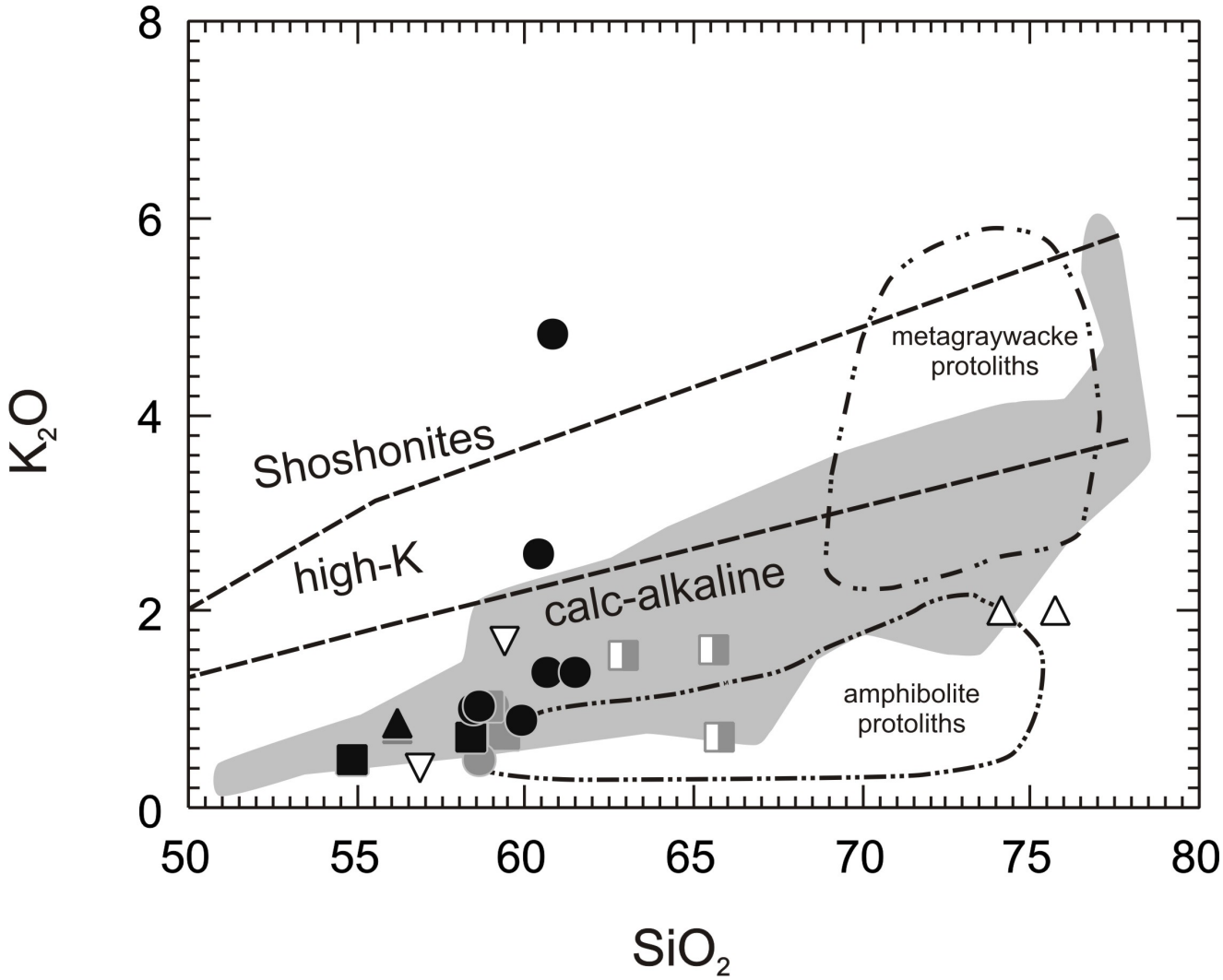

Figure KSi. K_2O – SiO_2 diagram for igneous rocks of the Snoqualmie quadrangle. Also plotted is a gray shaded field for 92 samples from the Snoqualmie batholith (Erikson, 1968, 1969) and the fields for water-undersaturated partial melts derived from amphibolite and metagreywackes as complied by Sisson and others (2003). Symbols are the same as in Figure TAS.

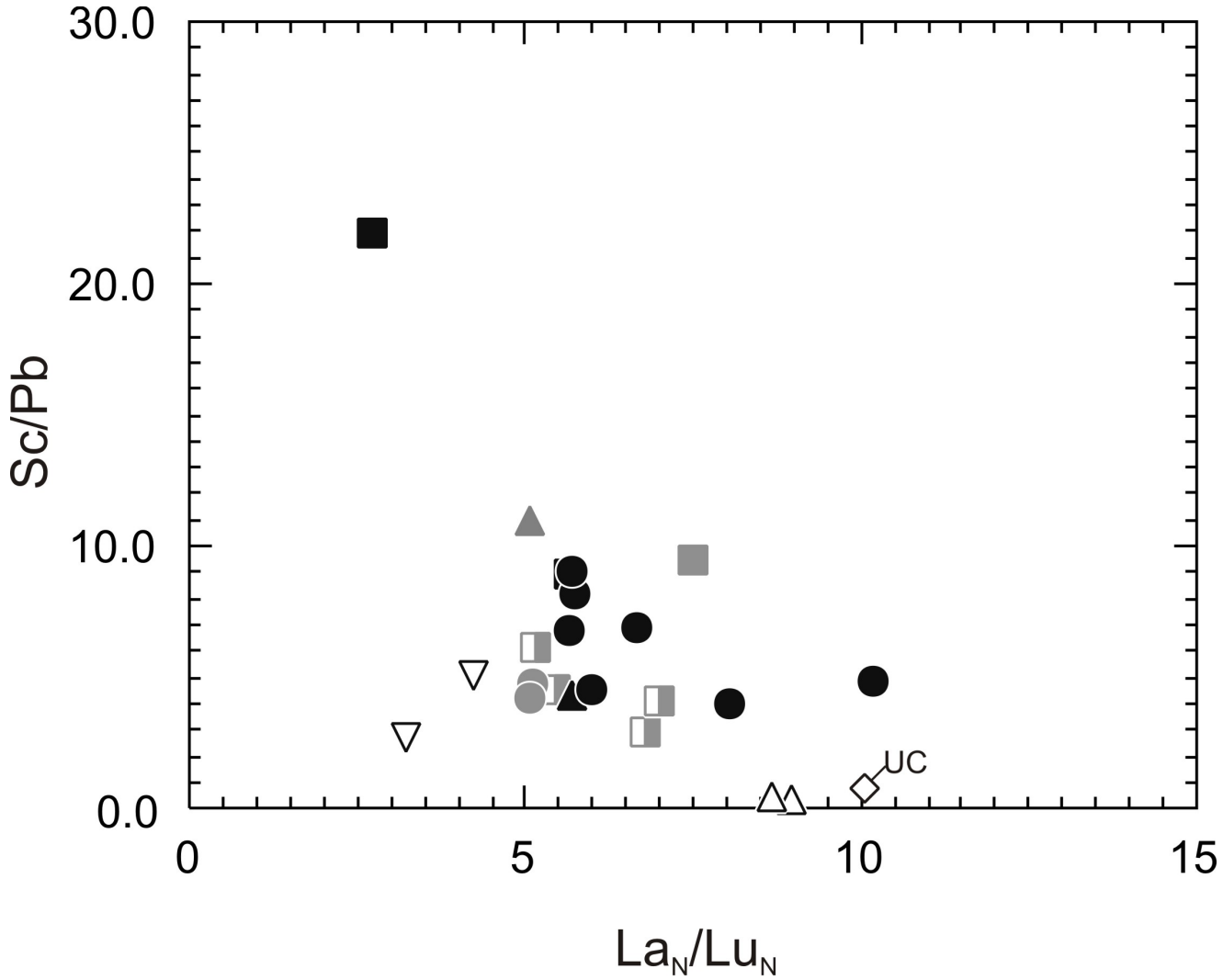

Figure ScPbLaLu. Sc/Pb vs. La/Lu normalized to chondrite values for the igneous rocks of the Snoqualmie quadrangle. Chondrite normalizing values from Sun and McDonough (1989). Also plotted is the average value of upper continental crust (UC) from McLennan (2001). Sc will be elevated in mafic rocks while Pb is an indicator of crustal assimilation. Symbols are the same as in Figure TAS.

Appendix 5. Deformation of Quaternary Deposits

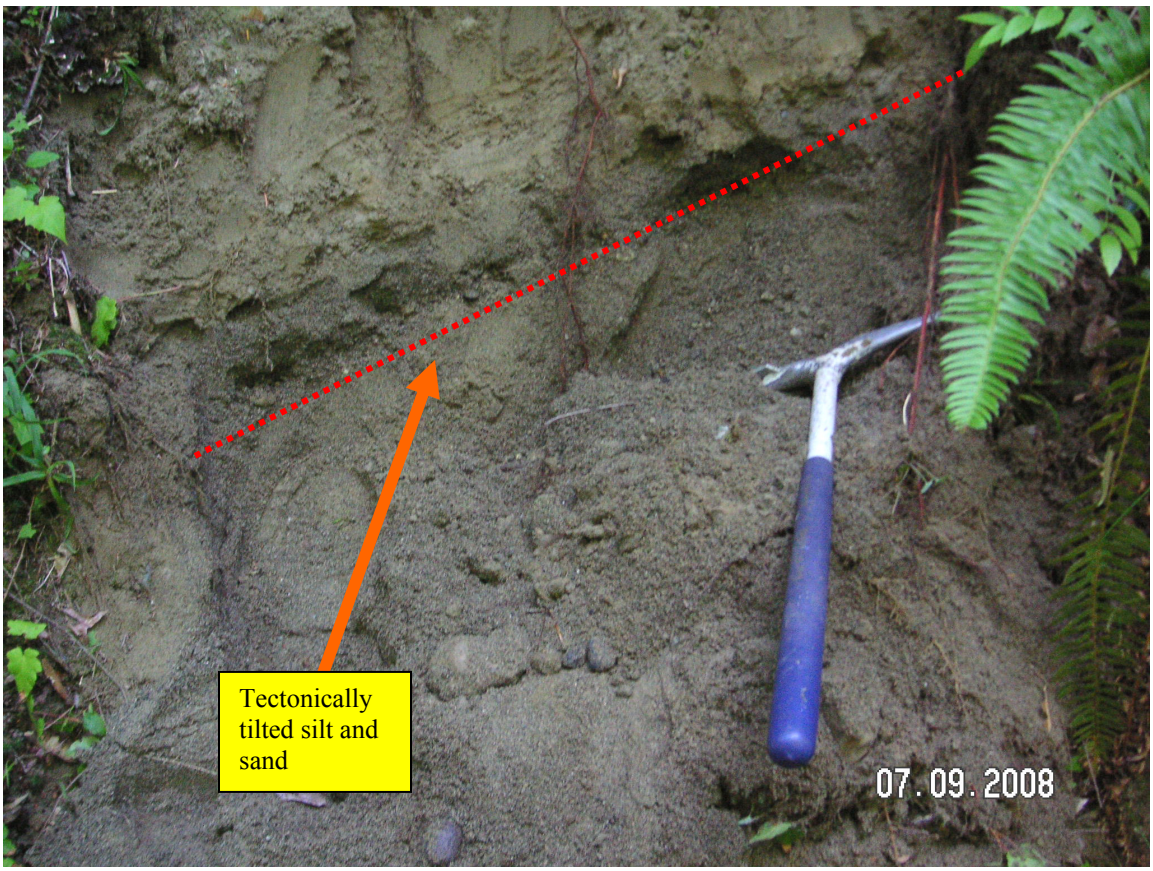

Figure 1. Site 08-4J
Olympia beds (unit Qc_o)

Tectonically tilted, thickly bedded, ancient Snoqualmie River alluvium (unit Qc_o) in the westernmost part of the Snoqualmie quadrangle and north of critical site and age date site 4M on plate 1 of Dragovich and others (2009a). Site is located near syncline and an unnamed fault on the western portion of cross section B on plate 2 of Dragovich and others (2009a) (NE¼SE¼ sec. 23, T24N R8E). Tectonic tilting may have been due to the nearby unnamed fault but is more likely tilted as a result of Quaternary folding. The bedding orientation here is consistent with the dip of other Olympia beds in the area and is the result of tectonic tilting. Photo shows dense, micaceous silt overlying coarse sand with some pebbles; also contains intermittent thin lenses of diamicton that may be ancient landslide deposits. Note geo-pick for scale. Beds (shown with dotted red line) strike 148° azimuthal and dip 15° NE. These sediments are exceptionally thick ancient Snoqualmie River alluvium that is now elevated, folded, and faulted within the Rattlesnake Mountain fault zone. Quaternary deformation at this site and in the North Bend quadrangle, as well as other geophysical, geomorphic, and lithologic anomalies, suggests that this area near Snoqualmie Ridge may be tectonically active.

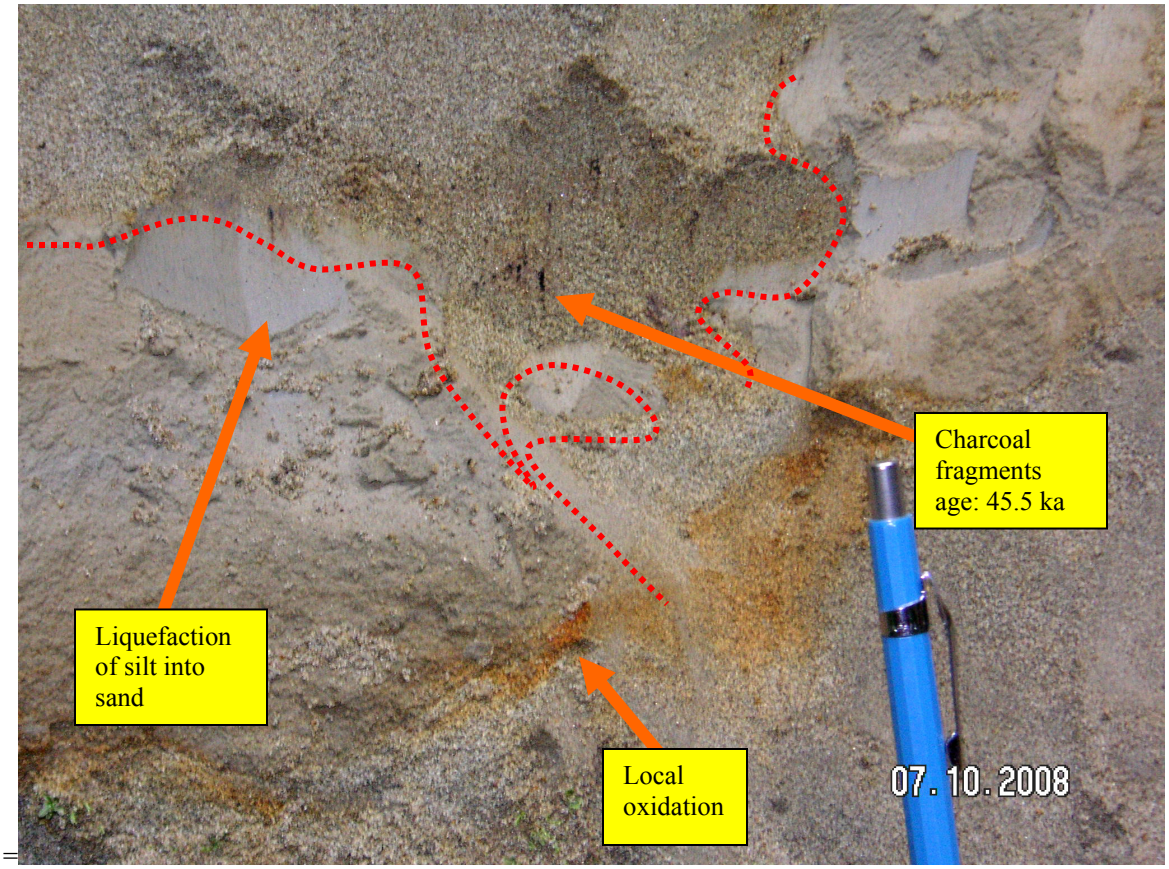

Figure 2. Site 08-4M
Olympia beds (unit Qc_o)

Critical site 4M on plate 1 of Dragovich and others (2009a), age date site (Table 1), and sand point count site (Appendix 1). Tectonically disrupted thin to thickly bedded Olympia beds with distinct liquefaction features. This ancient Snoqualmie River alluvium (unit Qc_o) is located in the westernmost part of the study area near a syncline and an unnamed fault. Site located SE¼SE¼ sec. 23, T24N R7E, on plate 1 of Dragovich and others (2009a). Photo shows bedded, dense, oxidized, laminated, micaceous silt and sand with distinct liquefaction features (outlined with dotted red lines). Disseminated charcoal pieces were found in Qc_o and were radiocarbon dated with the age of 45,540 ±930 B.P. (Table 1; cross section B on plate 2 of Dragovich and others [2009a]). Beds strike 322° to 327° azimuthal and dip 6° to 18° NE, respectively. Quaternary deformation at this site and in the North Bend quadrangle, as well as other geophysical, geomorphic, and lithologic anomalies suggest that faults in this area may be tectonically active. See following photo. These sediments are exceptionally thick ancient Snoqualmie River alluvium that is now elevated, folded, and faulted within the Rattlesnake Mountain fault zone. The Olympia beds, unit Qc_o, on Snoqualmie Ridge provide the best example of an inverted basin. Note pencil for scale.

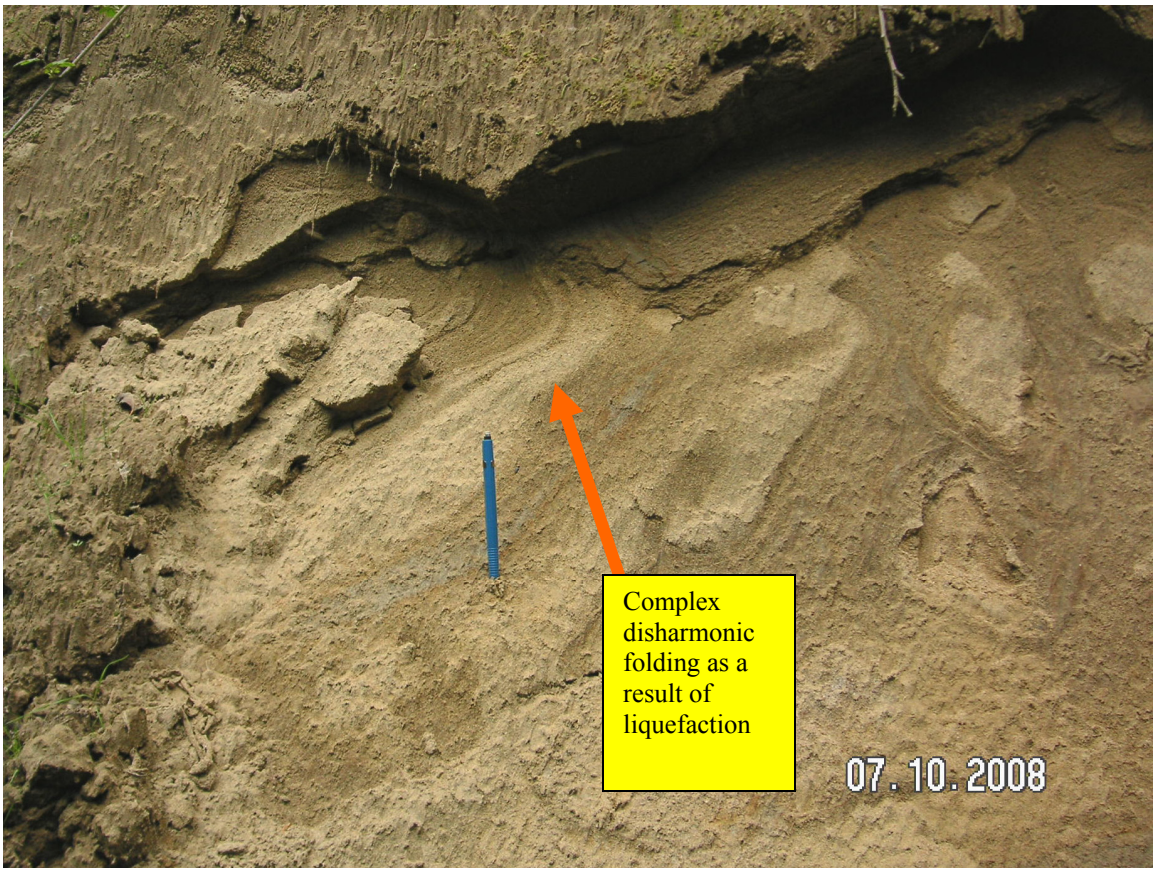

Figure 3. Site 08-4M
Olympia beds (unit Qc_o)

Critical site, age date site (Table 1), and sand point count site (Appendix 1) 4M showing the complex folding of silt and sand beds as a result of liquefaction. This disturbed, thin to thickly bedded ancient Snoqualmie River alluvium (unit Qc_o) is located in the westernmost part of the study area. Site is located on plate 1 of Dragovich and others (2009a) at SE¼SE¼ sec. 23, T24N R7E, near a syncline and an unnamed fault on the western portion of cross section B on plate 2 of Dragovich and others (2009a). Photo shows disharmonic folding of dense, contorted micaceous silt and sand beds with intense liquefaction features. Beds vary from laminated to thinly bedded; tannish color is characteristic of the ancient Snoqualmie River alluvium. Note pencil for scale.

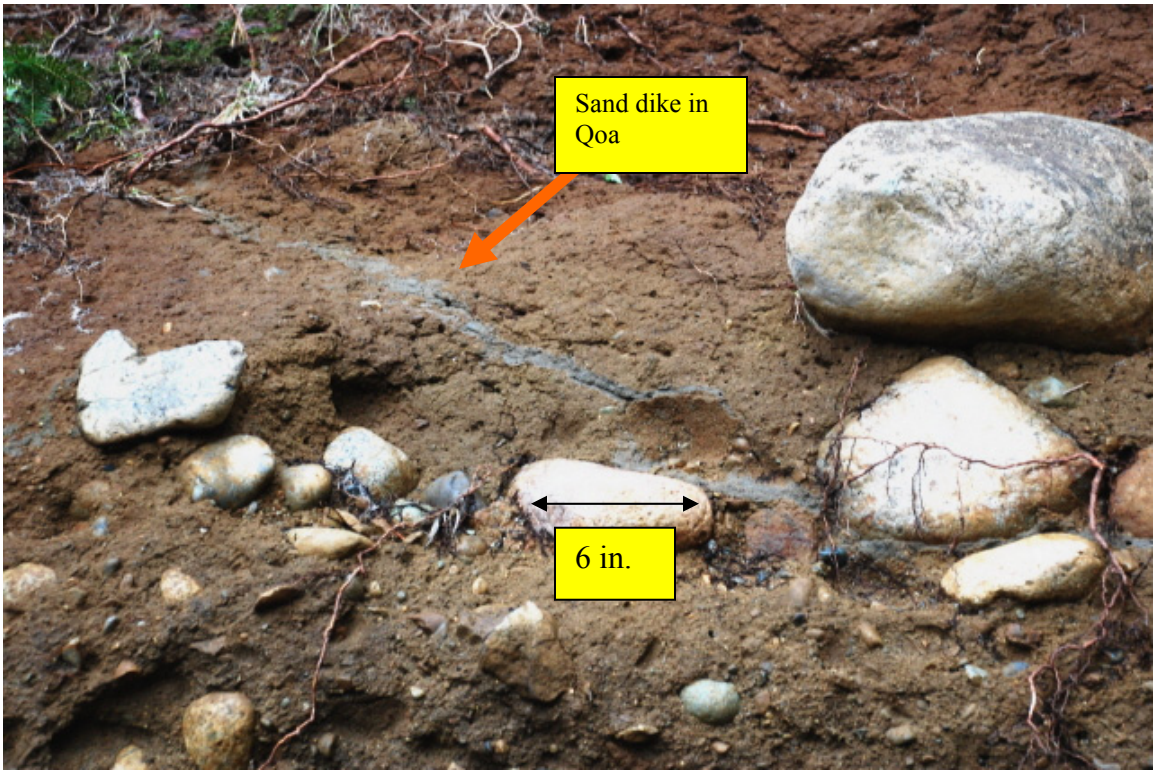

Figure 4. Site 08-9V
older alluvium (unit Qoa)

Critical site 9V on plate 1 of Dragovich and others (2009a). Tectonically disturbed old Snoqualmie River alluvium (unit Qoa) in the western part of the study area along Snoqualmie River. We cannot discount the possibility that this cobbly gravel is not a glacial outwash deposit but the stratigraphic position and only moderate density suggests older Snoqualmie River alluvium. Note old outwash (unit Qgo_p is found slightly lower in elevation in an outcrop near this site. Site located north-northwest of the bend in cross section B on plate 2 of Dragovich and others (2009a) in the SE¼NE¼ of sec. 24, T24N R7E. Photo shows bedded, medium dense cobble and gravel in an oxidized coarse sandy matrix. Note the grey-blue, long diagonal sand dike composed of medium to fine sand. Unit Qoa sediments may be locally uplifted along strands of the Rattlesnake Mountain fault zone. This site is east of Rattlesnake Mountain fault no. 1 along a straight section of the Snoqualmie River. Note cobble for scale.

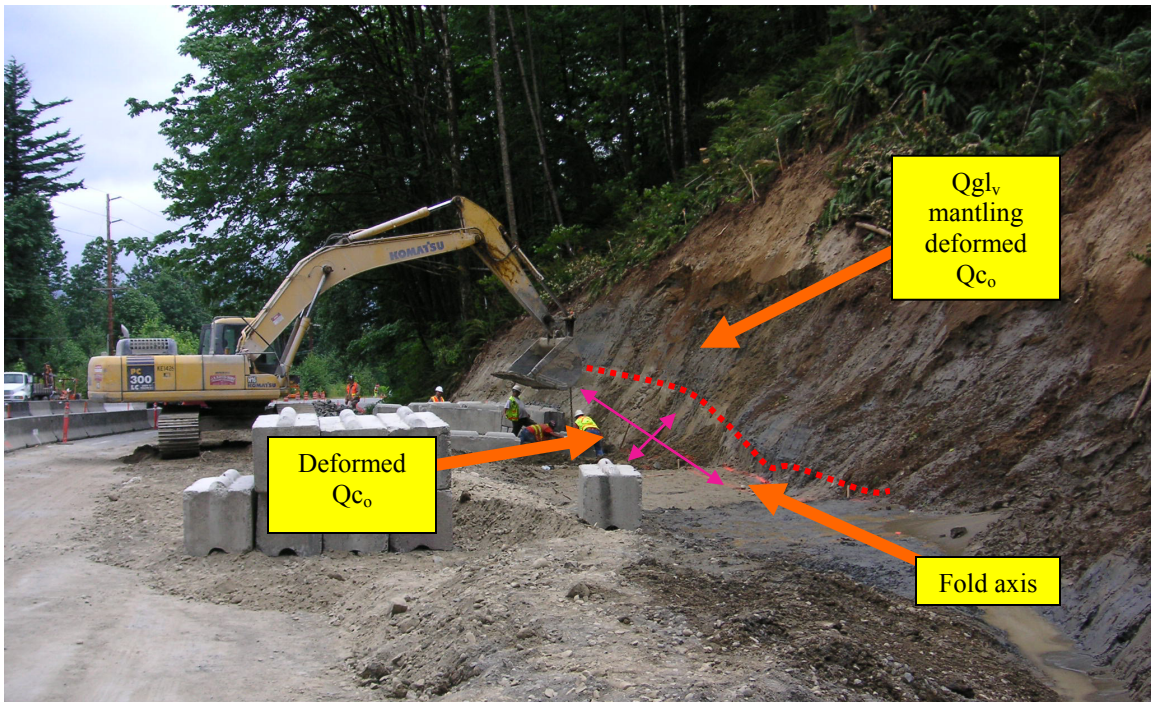

Figure 5. Site 08-13V
Vashon advance lake deposits (unit Qgl_v) on Olympia beds (unit Qc_o)

Critical site 13V on plate 1 of Dragovich and others (2009a). Tectonically tilted ancient Snoqualmie River alluvium (unit Qc_o) underlying advance glaciolacustrine deposits in the southwestern part of the study area. Site consists of dense, thickly laminated grey-blue silt (unit Qgl_v) overlying tilted oxidized tan silt and sand. Site located at Snoqualmie Casino roundabout on SE North Bend Way at SW¼SW¼ sec. 31, T24N R8E, near Rattlesnake Mountain fault no. 11B. Olympia beds strike 70° azimuthal, dip 24° SW, and likely define the nose of a SSE-plunging anticline. Advance lake deposits unconformably overlie the Olympia beds here above an angular unconformity. These lake deposits are locally tectonically fractured. Unit Qc_o (ancient Snoqualmie River alluvium) is elevated, folded, and faulted within the Rattlesnake Mountain fault zone. Quaternary deformation at this site and in the North Bend quadrangle, as well as other geophysical, geomorphic, and lithologic anomaliess suggests that this area near SE North Bend Way may be tectonically active. Note the outline of the contact between Qc_o and Qgl_v, the fold axis, and the workers for scale.

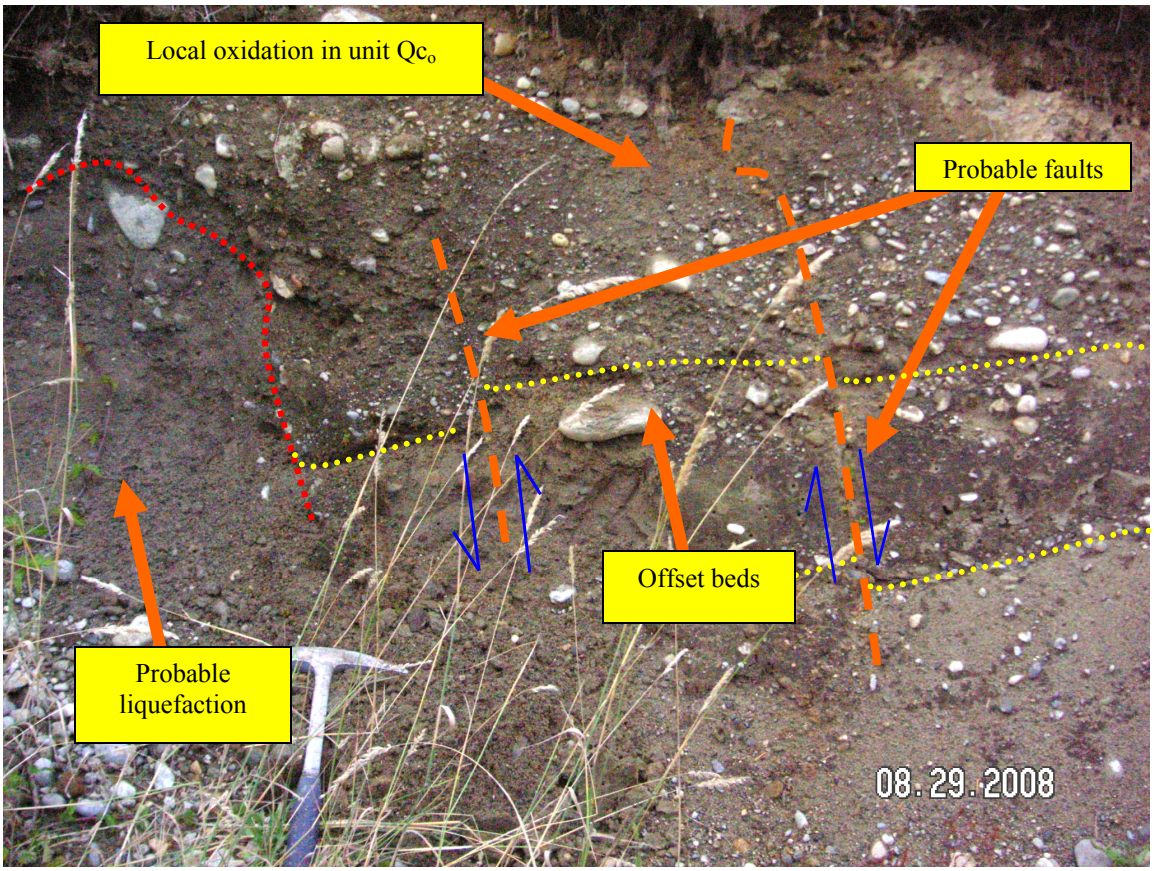

Figure 6. Site 08-29L
Olympia bed channel deposits (unit Qc_{oc})

Critical site 29L on plate 1 of Dragovich and others (2009a) and sand point count 29L-1 (Appendix 1) located at NW¼SW¼ sec. 31, T24N R8E, in an abandoned sand and gravel pit. The site is south of age site 11L on plate 1 of Dragovich and others (2009a) in the southwest part of the Snoqualmie 7-5 minute quadrangle. These ancient Snoqualmie River channel deposits are faulted. This probable tectonic deformation may be associated with a nearby anticline situated in between Rattlesnake Mountain fault no. 11A and B or may be related of poorly understood transfer fault between Rattlesnake Mountain faults no. 11A and 11B (see cross section B on plate 2 of Dragovich and others [2009a]). Beds (yellow dotted lines) strike 28° azimuthal and dip 10° SE. Faults (orange dashed lines) strike 255°to 260° azimuthal and dip 78° to 80° NW, respectively. Note the outline of a probable liquefaction feature (red dotted line) and offset beds between the faults. Geo-pick for scale. Quaternary deformation at this site and in the North Bend quadrangle, as well as other geophysical, geomorphic, and lithologic anomalies, suggests that this area around Rattlesnake Mountain fault no. 11A and B may be tectonically active.

Figure 7. Site 08-31B
Olympia beds (unit Qc_o)

Critical site 31B on plate 1 of Dragovich and others (2009a) located west of age date site 31C on plate 1 of Dragovich and others (2009a) at SW¼NW¼ sec. 30, T24N R8E. Area is in the southwest part of the study area near Rattlesnake Mountain fault no. 1 and near the bend in cross section B on plate 2 of Dragovich and others (2009a). Tectonically disturbed ancient Snoqualmie River alluvium (unit Qc_o) outcrop displays tilted bedding and incipient silt flames. Olympia beds are composed of thin convolute laminated silt beds displaying distinct flame structures surrounded by well-stratified thin- to medium-bedded sand to pebbly gravel. Beds strike 165°, 181°, and 216° azimuthal and dip 21°SE, 5°SW, 34° SW respectively. Note the tectonically tilted beds, distinct flame, and convolute lamination in the silt bed. Geo-pick handle for scale. Quaternary tectonic tilting and broad folding may have been due to the nearby Rattlesnake Mountain fault no. 1. Quaternary deformation at this site and in the North Bend quadrangle, as well as other geophysical, geomorphic, and lithologic anomalies, suggests that this area near Rattlesnake Mountain fault no. 1 may be tectonically active.

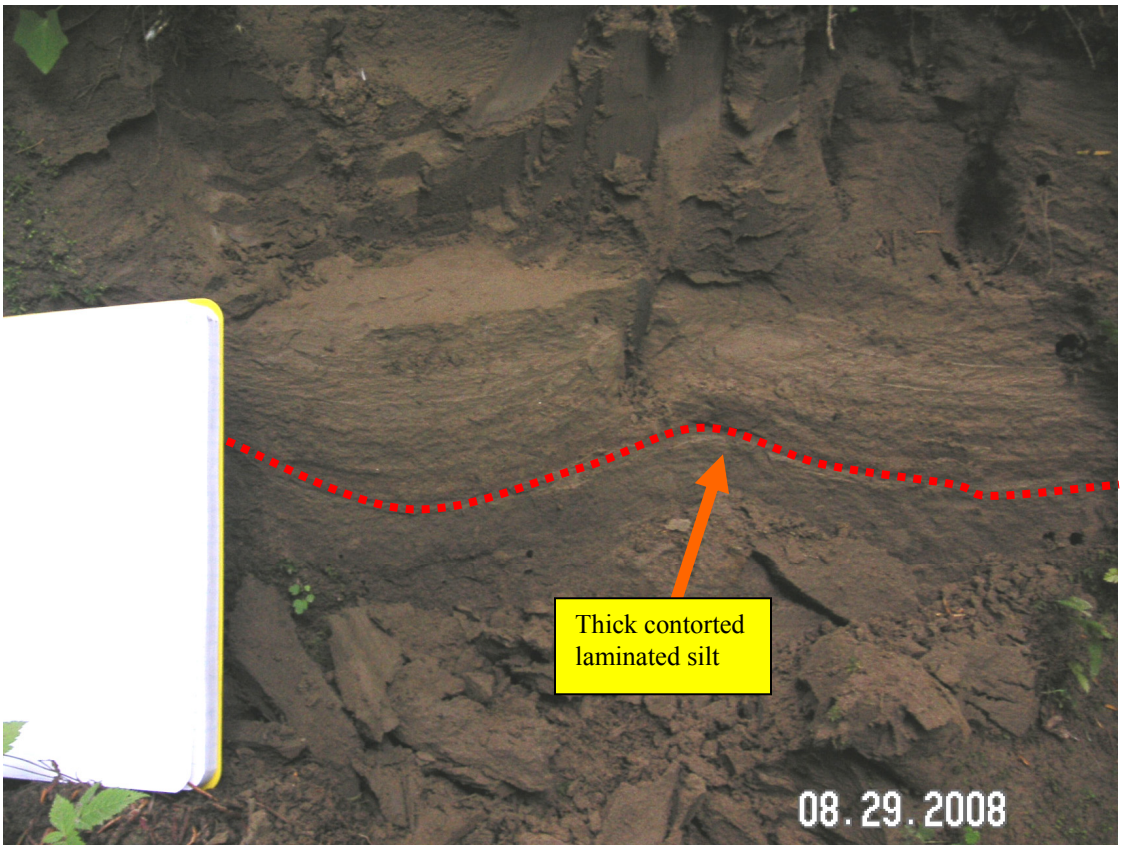

Figure 8. Site 08-31C
Olympia beds (unit Qc_o)

Critical site 31C on plate 1 of Dragovich and others (2009a) located in SW¼SW¼ sec. 30, T24N R8E, near RMF no. 1 and bend in cross section B on plate 2 of Dragovich and others (2009a). Ancient Snoqualmie River alluvium (unit Qc_o). (See sand point count data for site 31C in Appendix 1.) Beds here contain scattered small charcoal fragments in small lenses of medium sand; beds are very dense, thin to medium bedded, and are mostly micaceous silt to fine sand. The charcoal fragments were radiocarbon dated with the "infinite age" of >43,870 yr B.P. (See Table 1.) Beds strike between 141° to 147° azimuthal and dip 9° to 13° SW, respectively. We cannot discount fluvial wave ripples due to the symmetry of the structure, although lack of cross bedding suggests tectonic deformation. Flame structures are found in beds near the photo. Note the broad contorted lamination and the field book for scale. The Olympia beds are exceptionally thick ancient Snoqualmie River alluvium that is now elevated, folded, and faulted within the Rattlesnake Mountain fault zone. Quaternary tectonic tilting may have been due to the nearby near Rattlesnake Mountain fault no. 1, which may be tectonically active.

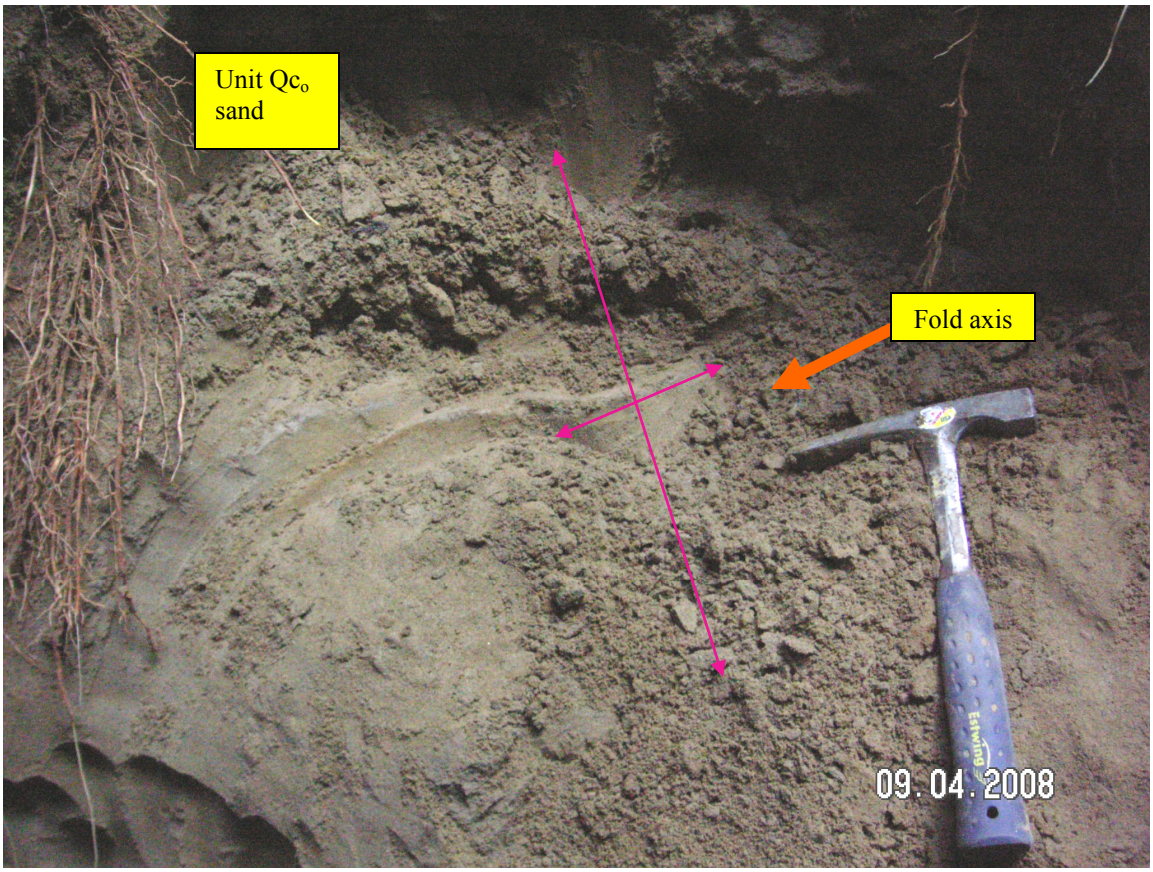

Figure 9. Site 08-35B
Olympia beds (unit Qc_o)

Critical site 35B on plate 1 of Dragovich and others (2009a) located in the SE¼NE¼ sec. 25, T24N R7E, in the southwest part of the study area between Rattlesnake Mountain fault nos. 1 and 11A. Tectonically disturbed glacial till (unit Qgt_v) (not shown here) overlying ancient Snoqualmie River alluvium sand (unit Qc_o) displaying liquefaction structures. Unit Qga_v is missing here between Qgt_v and Qc_o. Site consists of thin to thickly laminated silt to fine sand. Directly west of this outcrop, site 11L yielded a radiocarbon age of >44,020 yr B.P., which is similar to age date 31C of >43,870 (Table 1). The bedding orientation here is consistent with the dip of other Olympia beds near the site, indicating tilted panels of strata on a fold limb. Quaternary deformation at this site and in the North Bend quadrangle, as well as other geophysical, geomorphic, and lithologic anomalies, suggests that this area near Rattlesnake Mountain fault no. 1 may be tectonically active. Fold axis trends 185° and plunges 40° SSW. Note the fold axis and tectonically deformed and folded silt and sand. Rock hammer for scale.